Wilson, P.A., Lyle, M., and Firth, J.V. (Eds.)
Proceedings of the Ocean Drilling Program, Scientific Results Volume 199

1. Leg 199 Synthesis: Evolution of the Equatorial Pacific in the Early Cenozoic[1]

Mitchell Lyle[2] and Paul A.Wilson[3]

ABSTRACT

Ocean Drilling Program Leg 199, the first paleoceanographic leg in 30 years to target the Paleogene equatorial Pacific, had three primary objectives. First, the drilling was designed to develop modern age models and cross-calibrate biostratigraphy, magnetostratigraphy, isotope stratigraphy, and physical stratigraphy of the equatorial Pacific in order to form a chronologic framework of events. Second, specific intervals were targeted to constrain important paleoceanographic change. Three boundaries were targeted in particular: the Paleocene/Eocene (P/E) boundary, Eocene/Oligocene (E/O) boundary, and the late Oligocene and Oligocene/Miocene (O/M) boundary. Third, comprehensive time series studies were carried out on long intervals of Paleogene core to understand the long-term evolution of the equatorial Pacific, including changes in productivity, marine chemistry, temperature, and ice volume. The scientific goals were achieved through a drilling transect that crosses the position of the 56-Ma Pacific equator with an additional drill site (Site 1218) located at the 40-Ma Pacific equator.

INTRODUCTION

The modern Pacific Ocean, the largest ocean basin, occupies slightly more than 50% of modern global ocean surface area but accounted for almost 65% of total ocean area at the beginning of the Cenozoic. It has been a large medium-term reservoir of heat, carbon, and nutrients for the entire Cenozoic and is a major locus of carbon cycling to and from

[1]Lyle, M., and Wilson, P.A., 2006. Leg 199 synthesis: Evolution of the equatorial Pacific in the early Cenozoic. *In* Wilson, P.A., Lyle, M., and Firth, J.V. (Eds.), *Proc. ODP, Sci. Results,* 199: College Station TX (Ocean Drilling Program), 1–39. doi:10.2973/odp.proc.sr.199.201.2006
[2]Center for Geophysical Investigation of the Shallow Subsurface, Boise State University, 1910 University Drive, Boise ID 83703 USA. Present address: Department of Oceanography, Texas A&M University, College Station TX 77843, USA.
mlyle@cgiss.boisestate.edu
[3]National Oceanography Centre, Southampton School of Ocean and Earth Science, Southampton SO14 3ZH, UK.

Initial receipt: 22 February 2006
Acceptance: 4 September 2006
Web publication: 27 September 2006
Ms 199SR-201

the ocean interior. For example, 20%–60% of total marine primary production occurs in the modern equatorial Pacific (Chavez and Barber, 1987), and ~1 Gt of carbon is exchanged from the ocean to the atmosphere annually through upwelling of CO_2-enriched subsurface waters (Chavez et al., 1999).

Pacific Ocean circulation, temperature, primary productivity, and chemistry have all changed radically over the Cenozoic. Earth cooled from the extreme warmth of the early Cenozoic to the dual-pole icecaps of the Pleistocene. Study of the Cenozoic equatorial Pacific provides an opportunity to understand how different Earth systems interact under different boundary conditions of global temperature and geography.

Leg 199 is one of a set of recent Ocean Drilling Program (ODP) drilling legs that target Paleogene and Mesozoic paleoceanography. During Leg 171B, a transect of sites was drilled in the subtropical western North Atlantic (Blake Nose). During Legs 181 and 189 sites were drilled around New Zealand and the Tasman Rise to study the evolution of Pacific deepwater circulation and the development of circulation through the Tasman Gateway. During Leg 198, a depth transect was drilled on the Shatsky Rise to study the Mesozoic and early Cenozoic tropical Pacific, and during Leg 207 a similarly aged sequence was drilled on the margin of Suriname, Demerara Rise, in the equatorial Atlantic. Leg 208, on Walvis Ridge, studied the evolution of the South Atlantic.

In this paper we summarize the research from the Leg 199 shipboard scientific party and their collaborators since the end of Leg 199 drilling in December 2001. The contributions range from the rigorously metric to the posing of more speculative hypotheses (e.g., from developing the first continuous oxygen isotope stratigraphy for the Oligocene in the Pacific [Wade and Pälike, 2004; Lear et al., 2004; Pälike et al., submitted (**N1**)] to the use of the geographic fixity of equatorial upwelling to explore Cenozoic Hawaiian hotspot movement [Parés and Moore, 2005]).

After a brief description of the setting of the Eocene Pacific and a synopsis of ODP Leg 199 drilling, we describe stratigraphic efforts during Leg 199. Then we summarize studies of the Eocene/Oligocene (E/O) boundary event and Oligocene, followed by an exploration of interactions between Greenhouse Eocene conditions and the carbon cycle. Finally, we examine the Paleocene/Eocene (P/E) boundary event, also known as the Paleocene/Eocene Thermal Maximum (PETM) (Zachos et al., 2001).

EARLY CENOZOIC GREENHOUSE AND LATE CENOZOIC ICEHOUSE

Leg 199 was designed to study the equatorial Pacific in the early Cenozoic. In particular, the leg was drilled to understand how the equatorial Pacific responded to warm early Cenozoic global climate and how biogeochemical and physical processes of the equatorial Pacific helped to contribute to global warmth. A secondary goal was to understand how the equatorial Pacific changed as ice sheets grew on Antarctica.

Earth experienced a generally warm climate prior to 33.6 Ma, termed the "Greenhouse world" (e.g., Miller et al., 1987), which lasted until just after the end of the Eocene (the Eocene/Oligocene boundary is currently dated at 33.7 Ma). An oxygen isotope event known as Oi-1 beginning at ~34 Ma marked the appearance of extensive permanent ice sheets on Antarctica and the beginning of the "Icehouse world" (Miller

et al., 1987; Zachos et al., 2001; Coxall et al., 2005). The brief Oi-1 glacial interval had a maximum advance now dated at 33.6 Ma (Coxall et al., 2005; Pälike et al., unpubl. data). Roughly half of the Cenozoic, then, was significantly warmer than modern conditions. Additional information about the Cenozoic evolution of the Pacific can be found in Lyle et al. (submitted [N2]). Carbon cycle changes over the Cenozoic are large in comparison with those of the Holocene or Pleistocene. The beginning of the Cenozoic was marked by atmospheric CO_2 concentrations perhaps 4 to 5 times higher than modern atmospheric CO_2, contributing to early Cenozoic Greenhouse conditions (Pearson and Palmer, 2000; Demicco et al., 2003; Royer et al., 2004). Somewhere near the end of the Eocene or beginning of the Oligocene, atmospheric CO_2 content began to drop to near-modern levels (Pagani et al., 2005) and may have been a driver for the Greenhouse–Icehouse transition at the Eocene/Oligocene boundary. It is not possible with current data to show that the E/O cooling was caused by greenhouse gases, but all proxies agree that atmospheric CO_2 levels were high in the Eocene but dropped to near modern values by the end of the early Miocene (Pagani et al., 1999; Pearson and Palmer, 2000; Royer, 2002).

Feedback mechanisms from the carbon cycle are probably needed to maintain warmer than modern conditions in the Eocene. A modified carbon cycle is also needed to maintain the high atmospheric burden of greenhouse gases prior to 34 Ma. Because atmospheric CO_2 and methane concentrations probably have varied by large factors over the Cenozoic, the Paleogene provides a useful testing ground to study greenhouse gases and climate at tectonic, orbital and climate "transient" timescales. Climate transients like the PETM (Kennett and Stott, 1991; Dickens et al., 1995; Norris and Röhl, 1999; Thomas, 2003; Thomas et al., 2003; Zachos et al., 2003, 2005) provide an important means to study how the Earth responds to large short-lived changes in greenhouse gas concentrations forced by the release of fossil carbon. Carbon cycle and climate responses to the periodic changes in insolation caused by orbital variations (Laskar et al., 2004; Pälike et al., 2004) provide a way to monitor climate sensitivity under altered base conditions.

THE PACIFIC OCEAN IN THE PALEOGENE

The Paleogene Pacific Ocean was connected to the other oceans differently than the modern Pacific (Fig. F1). Before 25 Ma the major passages to the Indian and Atlantic Oceans were found in the tropics rather than through the high southern latitudes. The Panama Gateway between the tropical Atlantic and Pacific did not disappear completely until ~3 Ma (Coates and Obando, 1996), whereas the tropical Indonesian Passage between the Indian and Pacific Oceans became significantly restricted at ~11.5 Ma (Kennett et al., 1985). The Southern Ocean passages began opening in the middle Eocene and opened deeply at the end of the Eocene and during the Oligocene. It is now widely accepted that the Tasman Passage became a significant connection between the Indian and Pacific Oceans at ~35.5 Ma (Stickley et al., 2004). In contrast, the timing of the opening of Drake Passage is a subject of ongoing debate. Drake Passage may have formed deepwater connections between the Atlantic and Pacific as early as 34–31 Ma (Latimer and Filippelli, 2002; Lawver and Gahagan, 1998, 2003; Livermore et al., 2005) or as late as 24–17 Ma (Barker, 2001; Pfuhl and McCave, 2005). Recently,

F1. Circulation and upwelling, p. 28.

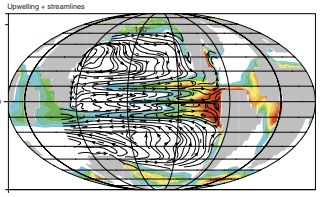

Scher and Martin (2006) suggest that significant connections through the Drake Passage were established as early as 41 Ma.

Modern mountain belts around the Pacific, which steer winds and define important loci of air-sea interactions, were markedly different in height and position at the beginning of the Cenozoic (Harrison et al., 1998; Chase et al., 1998). Nevertheless, Earth's energy balance at the top of the atmosphere appears to have been roughly the same at the beginning of the Cenozoic as it is today, and periodic changes in insolation were driven by changes in Earth's orbit and orientation with respect to the sun (Laskar et al., 2004; Pälike et al., 2004). Tectonic reorganizations by themselves were not the dominant cause of the different climates of the Cenozoic. Instead, the tectonic reorganizations affected climate by controlling the processes responsible for transporting or trapping solar heat and maintaining greenhouse gas levels in the atmosphere. The different climates of the Cenozoic provide natural experiments to understand interactions among the crust, oceans, atmosphere, cryosphere, and biosphere.

One result from modeling studies is that the basic structure of ocean circulation (i.e., the distribution of gyres and upwelling systems) seems to be recognizably similar to modern patterns (Huber and Caballero, 2003; Huber et al., 2003, 2004). The major exception is the disappearance of the Antarctic Pacific and Indian Ocean subpolar gyres with the Paleogene opening of the Southern Ocean gateways (Tasman Gateway and Drake Passage) (Huber et al., 2004). Another notable difference between the Paleogene and modern Pacific is a stronger interaction of the South Pacific subtropical gyre with that of the Indian Ocean. Although the general features of the Pacific Ocean are relatively constant, the position of fronts and other boundaries of circulation regimes may have moved by >5° in latitude over the Cenozoic (Huber and Sloan, 2001). In addition, the average temperature of the individual gyres is thought to have changed along with the cooling of the planet (Huber et al., 2004; Huber and Nof, 2006). Such changes in sea-surface temperature (SST) and position of these ocean heat reservoirs are important to the atmospheric redistribution of heat and precipitation (Huber and Sloan, 1999).

SYNOPSIS OF LEG 199 DRILLING

Eight sites were drilled during Leg 199 to study the Eocene (Table **T1;** Figs. **F2, F3;** see Lyle, Wilson, Janecek, et al., 2002, for more detail). Seven of these (Sites 1215, 1216, 1217, 1219, 1220, 1221, and 1222) were located on crust thought to be of late Paleocene age, to target the P/E boundary, also known as the PETM. Of these, Site 1216 was abandoned before reaching basement because of an extensive chert section encountered in the sediment section, and the age of basement was ambiguous at Site 1222. Sites 1217 and 1219 were situated on crust that was slightly too young to contain the P/E boundary section, but the P/E boundary interval was recovered at Sites 1215, 1220, and 1221. All of these sites contain important sediment columns dating from the early Eocene through the Oligocene. An additional site, Site 1218, was drilled on 42-Ma crust to study the late Eocene and the Eocene–Oligocene transition in more detail.

The sediments drilled across the Paleogene equatorial transect fall into the following five broad lithochronostratigraphic units (Fig. **F2**):

T1. Leg 199 drill sites, p. 38.

F2. Lithologic summary of Leg 199, p. 29.

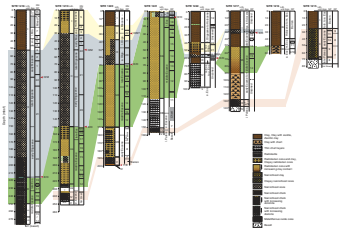

F3. Map of the central tropical Pacific, p. 30.

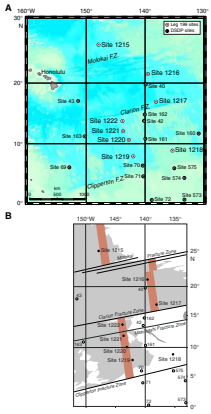

1. A surficial clay unit, sometimes containing a basal radiolarian ooze, with a basal age ranging from middle Miocene in the south of the transect (Site 1218) to early–middle Eocene in the north (e.g., Sites 1215 and 1216);
2. A nannofossil ooze/chalk unit whose base is at the E/O boundary and whose top is of early Miocene age in the south (Sites 1218 and 1219) and Oligocene age in the central part of the transect (Sites 1217, 1220, 1221, and 1222); Oligocene–Miocene carbonates are nonexistent in the north (Sites 1215 and 1216);
3. A middle–upper Eocene radiolarian ooze and radiolarian clay that is present at all sites except those in the north (Site 1215 and 1216);
4. A lower middle–lower Eocene unit composed of cherts, clays, and radiolarian ooze that is present in varying thicknesses at all Leg 199 sites along the 56-Ma transect except Site 1215 in the extreme north; and
5. A lower Eocene–upper Paleocene nannofossil ooze or chalk resting upon basalt basement that is recovered at all sites (except Site 1222, where cherts overlie basement, and Site 1216, where the relevant stratigraphic interval was not drilled).

Because of plate tectonics, each site drifted northwestward from the equatorial zone of high productivity as the crust aged. Sites 1215, 1216, and 1217 were always sited north of the equator, with Site 1215 found at ~12°N at the Paleocene/Eocene boundary, Site 1216 at 9°N, and Site 1217 at 5°N (see supplementary table of site positions in **Lyle et al.,** this volume). The remainder of the sites passed through the equatorial zone, ±2° of the equator. The position of the sites with respect to the paleoequator is fundamental to their lithologic history, and their northward passage out of the high-productivity zone is an important factor marking the top of the Oligocene–Miocene carbonates. The top of the carbonates occurs in the upper Miocene at the southern sites and in the Oligocene in the north. Periods when carbonates were deposited are also defined by global changes in the carbonate compensation depth (CCD) (Rea and Lyle, 2005; Shipboard Scientific Party, 2002), to be discussed in more detail later.

LEG 199 CONTRIBUTIONS TO PALEOGENE STRATIGRAPHY

Fundamental to all paleoceanographic studies are good age models to determine rates of change and age order of events at widely separate sites. The primary need of most paleoceanographic drilling legs is to tie newly recovered sediment columns into an accurate chronostratigraphy. The problem is compounded in the early Cenozoic because Paleogene reference chronostratigraphies are still in a reconnaissance stage. The early Cenozoic, until recently, has lacked recovery of good high-resolution continuous sediment sections on which orbital variations, paleomagnetic variation, and biostratigraphy can be measured. Postcruise studies of Leg 199 sediments have fundamentally advanced both our understanding of chronostratigraphy in the Paleogene tropical regions and our ability to intercalibrate different stratigraphic events by studying the continuous sections of lower Miocene through middle Eocene sediments recovered during the leg.

Magnetostratigraphy

Shipboard scientists were able to develop a continuous magnetostratigraphy from the Pleistocene to the middle Eocene on Leg 199 sediments (Lyle, Wilson, Janecek, et al., 2002; Lanci et al., 2004, 2005; Parés and Lanci, 2004). With this new paleomagnetic record it has been possible to intercalibrate paleomagnetic stratigraphy with equatorial Pacific biostratigraphy, cyclostratigraphy, and Paleogene isotope stratigraphy. Development of the continuous paleomagnetic record was possible because relatively undisturbed sediments were recovered during Leg 199 that had not been diagenetically altered to lose their initial magnetic signal. The equatorial sediment bulge has moved north over time, so relatively old sediment sections were not deeply buried, cemented, or strongly overprinted with diagenetic chemical signals. It was therefore possible to core Paleogene sections with the advanced piston corer and recover relatively undisturbed sediments amenable to paleomagnetic analysis. In addition, the sediments have remained oxidized throughout their history and preserve a good paleomagnetic signal.

Shipboard paleomagnetic measurements were good, making it easy to correlate between cores and assemble a shipboard paleomagnetic stratigraphy. However, postcruise U-channel studies significantly sharpened the record and allowed the search for short magnetic polarity reversals (Fig. F4) in the Miocene and Oligocene using records from Sites 1218 and 1219 (Lanci et al., 2004, 2005). Parés and Lanci (2004) continued the record on into the Eocene using Site 1220.

The high resolution of the U-channel paleomagnetic record allowed the search for short magnetic polarity changes, termed cryptochrons by Cande and Kent (1992, 1995). Interestingly, the high-resolution records from Sites 1218 and 1219 identified five short polarity reversal events but none that were of the age suggested by Cande and Kent (1995). Lanci et al. (2004, 2005) thus conclude that if the Cande-Kent cryptochrons exist, they must have lasted <5 k.y., the resolution of the Leg 199 records.

Both the shipboard and improved shore-based paleomagnetic stratigraphy provided the basis for recalibration of other stratigraphic datum levels and provided an initial age model for higher resolution cyclostratigraphic studies.

F4. Shipboard vs. U-channel VGP latitude, p. 31.

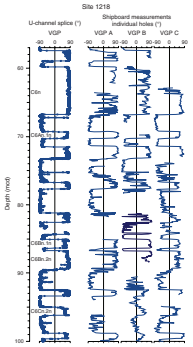

Biostratigraphy

Leg 199 provided the first intercalibration of paleomagnetic and radiolarian biostratigraphy for the entire Paleogene (Nigrini et al., this volume), and provided the first Oligocene low-latitude diatom biostratigraphy (also paleomagnetically intercalibrated; Barron et al., this volume). Recovery and analysis of upper Paleocene–lower Eocene carbonates also proved important to understand nannofossil biostratigraphy at the Paleocene/Eocene boundary (Raffi et al., 2005).

Radiolarians

Cenozoic tropical radiolarian stratigraphy was for the first time intercalibrated with paleomagnetic chronostratigraphy to radically revise zone boundary ages (Fig. F5) (Nigrini et al., this volume). Three different sites (1218, 1219, and 1220) were intercalibrated in age using paleomagnetic reversals and distinctive cyclical variations in physical properties. Biostratigraphic datum levels were established by their oc-

F5. Radiolarian zone ages/boundaries intercalibrated with magnetic reversal stratigraphy, p. 32.

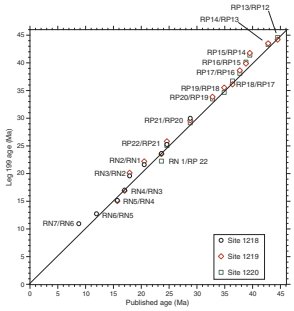

currence at the three different sites. Ages for 305 morphological first and last occurrences were established using paleomagnetics and cyclostratigraphy of the common data set. Ages for the established radiolarian zonation were then adjusted based on the new data. These new data allowed Moore et al. (2004) to develop modern age models for earlier Deep Sea Drilling Project (DSDP) drilling in the equatorial Pacific and explore changes in equatorial sedimentation through the Cenozoic.

Funakawa et al. (this volume, 2006) also studied radiolarian biostratigraphic datum levels in more detail around the Eocene/Oligocene boundary at Sites 1218, 1219, and 1220. **Kamikuri et al.** (this volume) performed detailed radiolarian counts around the Oligocene/Miocene boundary at Site 1219. Funakawa et al. (2006) note that the Eocene/Oligocene boundary is marked by large faunal turnovers and a large increase in cosmopolitan (probably cool water) forms. However, other radiolarian turnovers occurred in the late Eocene and early Oligocene. The E/O boundary appears to be the largest of several important events in this interval. **Kamikuri et al.** (this volume) note high variability in abundances of individual radiolarian species in the late Oligocene and early Miocene. These results suggest that important environmental information can be extracted with further study.

Diatoms

Similarly, the high-quality paleomagnetic stratigraphy of Site 1220 was used to intercalibrate low-latitude diatom stratigraphy for the interval between 33.5 and 21.5 Ma (Oligocene to early Miocene) (**Barron et al.,** this volume). Prior to Leg 199 the diatom datums had been calibrated to nannofossils, which were in turn calibrated to the paleomagnetic age model of Cande and Kent (1995). More than 35 new age estimates of diatom datum levels were assigned in this study.

Other Microfossils

Site 1219 provided an opportunity to establish an Eocene–Oligocene low-latitude silicoflagellate biostratigraphy (**Engel and McCartney,** this volume; **McCartney et al.,** this volume). Leg 199 was the first leg to study equatorial Eocene silicoflagellate biostratigraphy and was one of five that have investigated the Oligocene equatorial region. **Takata and Nomura** (this volume) also gathered new data on the abundance of benthic foraminifers in the Oligocene equatorial Pacific.

Detailed biostratigraphic studies across the Paleocene/Eocene boundary for benthic foraminifers (**Nomura and Takata,** this volume) and calcareous nannofossils (Raffi et al., 2005) add important new information to our understanding of equatorial biostratigraphy and bioevents around this important stratigraphic boundary. **Nomura and Takata** (this volume) counted time series of benthic foraminiferal assemblages across the Paleocene/Eocene boundary at Sites 1215, 1220, and 1221. In this preliminary study, they found that the last occurrence of Paleocene benthic foraminifers at Site 1221 occurs ~30 cm below the location of the carbon isotope event in the same core, rather than coincidental with it. They also found high abundances of benthic foraminifers in the two sites (1220 and 1221) near the Paleocene/Eocene equatorial position.

Raffi et al. (2005) conducted a detailed study of the Paleocene/early Eocene boundary primarily from Site 1215 to determine biostratigraphy, biochronology, and evolutionary history of nannofossil assemblages across this important event in the central equatorial Pacific.

Using carbonate cycles at Site 1215 they established a floating cyclostratigraphy (i.e., relative to the first appearance of *Tribrachiatus bramletti*) assuming that the carbonate cycles correlate to orbital variations in solar insolation. They then compared P/E intervals between the low-latitude Pacific and Atlantic Oceans and found almost identical sequences of evolutionary change in the two interconnected oceans.

Cyclostratigraphy

Cyclostratigraphic studies are extremely important to develop Cenozoic age models. These types of correlative stratigraphy allow development of high-resolution age models and better study of the timing of important paleoceanographic events. **Pälike et al.** (this volume) describe the first step in this process for Leg 199, development of an integrated stratigraphic correlation using Sites 1218 and 1219 and improving the spliced records at each site by revising the composite depth scale and stacking physical property records.

Better timescales than the shipboard age models based on magneto- and biostratigraphy are now being constructed by identifying cyclic variations of carbonate and correlating the cycles to age models of orbital variations. For example, Wade and Pälike (2004) correlated the refined Leg 199 physical property data with recently developed Paleogene orbital insolation models (Laskar et al., 2004) to develop an age model for the Site 1218 record between 26.4 and 30 Ma. They combined the new age model with stable oxygen and carbon isotope data reported in **Wade and Pälike** (this volume) to better date Oligocene glaciations and to investigate their relationship to longer period insolation variability. Pälike et al. (submitted [**N1**]) extended this correlation to the entire Oligocene using Site 1218 as the Oligocene reference section.

Cyclostratigraphy also helps to discriminate between alternate solutions for the evolution of planetary movements in the solar system (Pälike et al., 2004). Data from Sites 926, 929, and 1218 were used to search for a chaotic change from a 2:1 resonance to a 1:1 resonance for the 2.4- and 1.2–m.y. eccentricity modulations. One model (Laskar et al., 1993) predicted such a change some time after 30 Ma, whereas a newer model (Laskar et al., 2004) did not. The sedimentary records showed no evidence of such a change in signal since the Eocene/Oligocene boundary. Although this finding does not prove the Laskar et al. (2004) model, it is strong evidence that the Laskar et al. (1993) model is incomplete.

Seismic Stratigraphy

It is well known that the Neogene equatorial Pacific has a distinctive pattern of seismic horizons that extend for >1000 km (Mayer et al., 1985; Bloomer et al., 1995). These horizons mark large-scale changes in carbonate deposition (Mayer et al., 1985, 1986), and they extend over such large distances because of the size of the equatorial Pacific biome and the related scale over which coherent paleoceanographic changes occur. An example of the fine-scale coherence over large distances is the submeter correlation in physical properties that was possible between Sites 1218 and 1219, separated by ~740 km (**Pälike et al.,** this volume).

Lyle et al. (2002) showed that a distinctive seismic stratigraphy also exists for the Paleogene equatorial Pacific. Several Leg 199 researchers are working to tie seismic horizons to sedimentary horizons so that they may be used to study regional sedimentology (e.g., Mitchell and Lyle, 2005). The first-order problem is to compare a seismic response,

measured in two-way traveltime, to a change in physical properties measured in depth below seafloor. **Rea and Gaillot** (this volume) explored the problem of expansion of the sedimentary section caused by drilling and carrying the sediments from high subseafloor confining pressures to the ocean surface. They developed a new methodology to estimate rebound based on comparing thicknesses of distinctive density (or other physical properties) features between the logged interval and the multisensor track (MST) splice. This allows shipboard physical property measurements to be corrected for changes caused by depressurization of the sediment column.

Busch et al. (this volume) assessed the ability of shipboard measurements to predict acoustic impedance, needed for determining the seismic reflection profile. Their work was hampered by the lack of adequate velocity data from downhole logging. Corrections to produce in situ velocity from shipboard measurements were thus based on published relationships. Nevertheless, density variations proved to be very good predictors of acoustic impedance for seismic stratigraphy applications. For the equatorial Pacific, where carbonate content is a good predictor of density (e.g., Mayer, 1991), seismic reflection profiles can be used to estimate subsurface carbonate content.

Vanden Berg and Jarrard (2004, this volume) also showed how sediment composition could be estimated from physical property data from cores and used light absorption spectroscopy (Vanden Berg and Jarrard, 2002) to develop detailed downcore records of mineralogy. These records use more physical property information than just density but demonstrate two concepts—how mineralogical records of moderate accuracy can be quickly generated for a basic lithostratigraphy and how much of the mineralogical information is encoded in the physical properties of the bulk sediments. **Vanden Berg and Jarrard** (this volume) also found that density is always the strongest predictor for carbonate in their stepwise regressions.

PALEOGENE DISCOVERIES

The continuous Paleogene sedimentary sections from Leg 199 provide new opportunities to document and understand the Cenozoic evolution of the equatorial Pacific. These studies include understanding how productivity has changed, the timing of glaciations, and the involvement of long period-changes in orbitally driven insolation, timing and extent of rapid changes in climate state, and involvement of the carbon cycle in climate change.

Paleoproductivity and Plate Movement

Moore et al. (2004) used the newly updated ages of radiolarian zone boundaries to explore changes in equatorial Pacific productivity from the Paleocene to the late Miocene. Furthermore, Parés and Moore (2005) tracked northward Pacific plate movement by assuming that the linear sedimentation maximum found in each time slice from Moore et al. (2004) marks the position of the paleo-equator.

The modern Pacific equatorial zone has significantly higher productivity and higher biogenic sedimentation than other pelagic biomes (Murray et al., 1993; Honjo et al., 1995) (Fig. **F6**). Biogenic mass accumulation rates (MAR) between 0° and 1° north or south of the equator are ~50% higher than biogenic MAR between 1° and 2° north or south. Because the productivity is caused by Ekman divergence, a physical pro-

F6. Primary productivity vs. bulk MAR for the equatorial Pacific, p. 33.

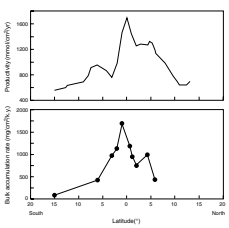

cess that is driven by the change in sign of coriolis force at the equator, there should always be upwelling at the equator as long as the trade winds blow from east to west (Wyrtki, 1981; Chavez et al., 1996) (Fig. F7). The nutrients added by upwelling deeper waters into the euphotic zone fertilize the equatorial region.

More than 90% of the sediments in the equatorial Pacific are biogenic in origin, so sedimentation rates are a semiquantitative proxy of paleoproductivity in the region. Moore et al. (2004) used these ideas to study the Cenozoic evolution of Pacific equatorial zone. The most striking discovery is of a secondary productivity zone in the northern tropical Pacific in the Eocene and early Oligocene. The secondary zone is probably associated with divergence at the boundary of the Eocene North Equatorial Current with the North Equatorial Countercurrent (Fig. F8) (Moore et al., 2004). Moore et al. (2004) also note that deposition of biogenic sediments in the equatorial sediment tongue varied by a factor of 2 to 5 in different time slices representing 5- to 6-m.y. averages. Such large variability, even when averaged over such long periods, makes it clear that large-scale variations of equatorial Pacific winds and upwelling have occurred as part of the evolution of the Cenozoic.

Moore et al. (2004) noted that the paleoposition of the equatorial sediment tongue did not always backtrack to an equatorial position. Parés and Moore (2005) used the misalignment of the equator backtracked via a stationary hotspot model of Pacific plate motion to explore the motion of the Hawaiian hotspot in the Cenozoic. They found a heartening agreement between "sedimentary" Pacific plate polar wander and Cenozoic poles estimated by other means (Tarduno et al., 2003) Through this method Parés and Moore (2005) were able to discern new detail of Cenozoic Pacific plate motion. The results support other data that indicate southward motion of the Hawaiian hotspot since the Cretaceous at a rate of ~32 km/m.y. and the general northward motion of the Pacific plate since 53 Ma of 12°, or ~25 km/m.y.

F7. Chlorophyll contents in the Pacific equatorial region, p. 34.

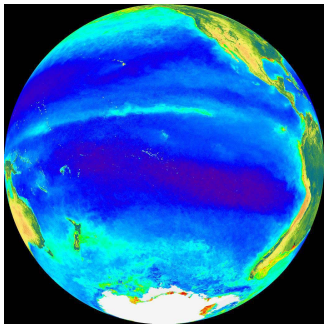

F8. Average late Eocene sedimentation rates in the tropical Pacific, p. 35.

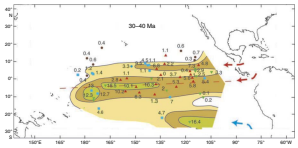

Oligocene

Arguably, the single most important paleoclimate rationale for ocean drilling is that deep-sea sediments provide the most stratigraphically complete and globally representative proxy records of global change. One of the outstanding highlights of Leg 199 was our recovery of stratigraphically complete sequences (the sections drilled are virtually free of hiatuses at the biostratigraphic zone and magnetochron level), representative of substantial tracts of the central Pacific Ocean. Undoubtedly, the most elegant demonstration of this important highlight is the detailed stratigraphic correlation of Oligocene sedimentary sequences, including the Eocene–Oligocene and Oligocene–Miocene transitions, recovered at Sites 1218 and 1219 (located nearly 750 km apart) to the decimeter level (**Pälike et al.,** this volume).

In many ways the Oligocene (~33.7–23.03 Ma) represents something of a "neglected middle child" of Cenozoic paleoceanography—caught between the early Paleogene Greenhouse and the well-developed Neogene Icehouse. This situation is at least partly attributable to the perception that the Oligocene marks a prolonged interval of relative stasis in paleoclimate and biotic turnover, as indicated in deep-sea micropaleontological communities by conservative body plans, confusing taxonomies, and low biostratigraphic resolution. However, in some respects the Oligocene represents the most interesting piece of the Cenozoic paleoceanographic puzzle because it offers an opportunity to unravel

the processes that lie behind the transition from a world free of large-scale continental icecaps and rapid eustatic sea level oscillations to one dominated by these climatic changes. Recent progress in our understanding of Oligocene paleoclimates has largely been driven by seismic stratigraphy and scientific drilling on continental margins (e.g., Browning et al., 1996; Miller et al., 1996; Pekar et al., 2002). In contrast, benthic stable isotope compilations (e.g., Miller et al., 1987; Zachos et al., 2001) show that paleoclimate records for the deep oceans through the Oligocene rely heavily on old DSDP sites, largely from the Atlantic Ocean (Miller et al., 1987, 1988, 1990, 1991, 1993), with a relatively low sample spacing. Leg 199 presented an excellent opportunity to generate low-latitude deep-sea records throughout the Oligocene in order to test models developed from continental margin sequences for the pattern and timing of changes in global temperature and continental ice volume.

Previous studies designated "Oi events" in the Oligocene to represent transient glaciations based on intervals where particularly heavy oxygen isotope ratios were observed in relatively low resolution data sets from several sites (e.g., Miller et al., 1991). High-resolution (up to 2 k.y.) Oligocene stable isotope stratigraphies now exist for bulk sediment (top Subchron C6An.2n through base Subchron C6Cn.3n; most of Chron C9n; top Chron C12n through base Chron C13n), planktonic (top Chron C9n through base Subchron C11n.1n), and benthic foraminiferal calcite (the entire Oligocene, including the E–O and O–M transitions) from Site 1218 (Wade and Pälike, 2004; Coxall et al., 2005; **Tripati et al.,** this volume; **Pälike et al.,** submitted [**N1**], this volume). These new data sets from Site 1218 demonstrate pronounced cyclicity in the orbital bands and shed new light on the Oi events. It is now clear that such events occur more regularly than previously supposed and are characterized by higher amplitude $\delta^{18}O$ change at orbital timescales as well as regular cyclic behavior in $\delta^{13}C$ records, predominantly with a 405-k.y.-long eccentricity spacing. In fact, the new data sets have made it possible to develop a new naming scheme for Oligocene glacial maxima that is based on the 405-k.y. eccentricity cycle count (Wade and Pälike, 2004), avoiding some of the confusion caused by previous conflicting naming schemes. The occurrence of these glacial maxima is striking because intervals with the highest $\delta^{18}O$ values consistently correspond to obliquity minima modulated with a period of 1.2 m.y. (and triggered to minima in the ~405 and ~100 k.y.) eccentricity cycles (Wade and Pälike, 2004; Coxall et al., 2005; Pälike et al., submitted [**N1**]). This important result supports the view that seasonality plays a key role in determining the development of glacial maxima. Specifically, the key factor in the development of the major Oligocene glaciations is not the occurrence of particularly cold winters or the occurrence of particularly cold summers but rather the prolonged absence of particularly warm (Southern Hemisphere) summers.

Two methods have been employed to help quantify the magnitude of Antarctic ice volume and thus sea level change during the Oligocene using Site 1218 sediments. Where both benthic and planktonic $\delta^{18}O$ records are available (top Chron C9n through base Subchron C11n.1n), sea level changes of up to 60 m have been estimated from benthic $\delta^{18}O$ data on the basis that ice volume fluctuations cannot exceed the variation recorded in paired planktonic data (Wade and Pälike, 2004). The other method is to use paired Mg/Ca and $\delta^{18}O$ data in benthic foraminifers to calculate seawater $\delta^{18}O$ (sw) (Lear et al., 2000). Application of

this method to the Site 1218 section suggests that a large Antarctic ice sheet formed during Oi-1 and subsequently fluctuated throughout the Oligocene on both short (<0.5 m.y.) and long (2–3 m.y.) timescales, between ~50% and 100% of its maximum earliest Oligocene size (consistent with estimates of sea level derived from sequence stratigraphy) (Lear et al., 2004).

Site 1218 $\delta^{13}C$ stratigraphies for the Oligocene also demonstrate pronounced cyclicity in the orbital bands with a particularly strong imprint of the ~405-k.y. eccentricity cycle, indicative of changes in global carbon burial. Where both benthic and planktonic records are available, we see that alterations of high-latitude temperatures and Antarctic ice volume had a significant impact on equatorial productivity (Wade and Pälike, 2004). Cross-spectral analysis of the Site 1218 Oligocene stable isotope data sets indicates a complex pattern of lead-lag relationships. Benthic $\delta^{18}O$ lags $\delta^{13}C$ in the early Oligocene, corresponding to ~8 k.y. in the 40-k.y. band. The lag suggests that the response of the global carbon cycle to Earth's obliquity helped to force changes in ice volume and high-latitude temperature (Coxall et al., 2005). For the entire Oligocene, an ~20-k.y. lag of $\delta^{13}C$ compared to $\delta^{18}O$ is found for the long eccentricity (405 k.y.) cycles suggesting that, in turn, changes in Antarctic ice volume and high-latitude temperature had a significant impact on global carbon cycling, and ocean buffering of the global carbon cycle (Pälike et al., submitted [**N1**]).

Eocene/Oligocene Boundary

The Eocene–Oligocene transition represents a pivotal point in the transition from the Greenhouse world of the Cretaceous and early Paleogene into the late Paleogene–Neogene Icehouse. Yet, the rarity of complete deep-sea sections across this interval has limited our understanding of the dynamics of this important step leading to the modern Icehouse world.

The Eocene–Oligocene transition is marked by a large rapid increase in the benthic foraminiferal calcite $\delta^{18}O$ record in earliest Oligocene time (Oi-1). This excursion was first ascribed to a 5°C temperature drop, but more recently Oi-1 has been associated with the onset of continental ice accumulation on Antarctica (Shackleton and Kennett, 1975; Shackleton, 1986; Miller et al., 1987, 1991; Zachos et al., 1992). Such confusion reflects the long-standing difficulty of separating the effects of temperature and ice on benthic $\delta^{18}O$ (Lear et al., 2000) and thus the relative importance of cooling vs. higher Antarctic snowfall. A benthic Mg/Ca record for the E/O transition from DSDP Site 522 (South Atlantic) shows no significant change corresponding to "Oi-1," suggesting that all of the $\delta^{18}O$ increase associated with Oi-1 can be ascribed to ice growth with no concomitant decrease in polar temperatures (Lear et al., 2000). Support for this suggestion exists from modeling experiments and sedimentary records (Kohn et al., 2004; Grimes et al., 2005). According to these data, the trigger for continental glaciation lay in the hydrological cycle rather than the carbon cycle. Specifically, it has been proposed that the opening of the Australian-Antarctic Seaway in earliest Oligocene time might have enhanced the supply of moisture as snow to the Antarctic interior (Lear et al., 2000). On the other hand, paleoproductivity studies suggest that the near-contemporaneous increase in seawater $\delta^{13}C$ was driven by increased rates of C_{org} burial in marine sed-

iments, and this factor may be implicated in global cooling and ice sheet growth (Diester-Haass and Zahn, 2001).

Even if global cooling did not trigger Cenozoic Antarctic glaciation, some of the feedback processes associated with the development of a large ice sheet might be expected to cause cooling. Either way, long-standing global lithologic compilations indicate a pronounced deepening of the CCD near the Eocene–Oligocene transition (van Andel et al., 1975; Delaney and Boyle, 1988) that has not been studied in detail.

Until recently, our most complete records of the E/O boundary came from two mid-latitude sites, both in the Southern Hemisphere (DSDP Site 522 and ODP Site 744). Leg 199 radically improved our archive of deep-sea sections across this important climate transition by recovering E/O boundary sections from five Northern Hemisphere sites (1217, 1218, 1219, 1220, and 1221). Taken together, these sites provide a valuable opportunity to study the chain of events across the E/O boundary within the framework of a depth and latitudinal transect. Throughout this transect, the transition from the Eocene to the Oligocene is instantly recognizable by a sharp upsection shift from SiO_2-rich and carbonate-poor to carbonate-rich and SiO_2-poor sediments. Shipboard observations indicated that the CCD deepened substantially, rapidly, and permanently across the Eocene–Oligocene transition (Fig. F9, from Shipboard Party, 2002). One objective of postcruise research was to quantify this relationship.

Coxall et al. (2005) generated high-resolution (up to 2 k.y.) records of percent (and mass accumulation rate) $CaCO_3$ and benthic $\delta^{18}O$ and $\delta^{13}C$ for the E–O transition at Site 1218. These data show that the CCD deepening across the E–O transition occurred much faster than previously documented, occurring in two jumps of about 40-k.y. each, separated by a ~200-k.y. "plateau." Remarkably, this deepening occurred synchronously with the stepwise onset of Antarctic ice sheet growth, as indicated by the parallel increase in the $\delta^{18}O$ series (Coxall et al., 2005). Ultimately, the trigger for these events is interpreted to have been an orbital configuration favoring the prolonged absence of warm Antarctic summers (low eccentricity and low-amplitude obliquity change) (Coxall et al., 2005). Yet, some additional conditioning factor must have been at work because there is no evidence that the low-eccentricity obliquity "node" conditions at 34 Ma were any more extreme than those that occurred regularly during preceding Eocene time (Coxall et al., 2005). A likely candidate for this climate conditioning factor is long-term decline in atmospheric carbon dioxide (e.g., DeConto and Pollard, 2003). The amplitude of $\delta^{18}O$ increase in the Site 1218 data is three times larger than that modeled by DeConto and Pollard (2003) and impossibly large to be explained by ice growth on Antarctica alone (Coxall et al., 2005). This important observation raises the intriguing possibility that Northern Hemisphere glaciation was initiated much earlier than widely believed. Alternatively, the data can be explained by concomitant global cooling (by ~4°C). This alternative calls into question a diverse range of data sets, including benthic Mg/Ca records, that show little evidence for cooling across the E/O boundary. Lear et al. (2004) present a Mg/Ca record for the E–O transition at Site 1218 and compare it to the one generated at DSDP Site 522 by Lear et al. (2000). This analysis, together with work on the sensitivity of Mg partitioning between seawater and benthic foraminiferal calcite, suggests that some other factor (e.g., pH or $[CO_3^{2-}]$) acts to partially mask the cooling signal in the Mg/Ca records for the E–O transition.

F9. Subsidence histories for nonequatorial and equatorial Leg 199 sites, p. 36.

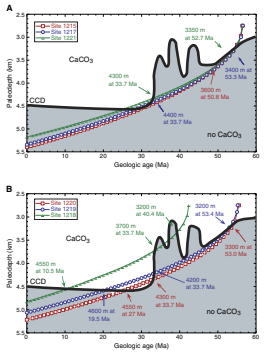

The "lock-step" behavior of the $\delta^{18}O$ and CCD records for the E–O transition at Site 1218 suggests that ocean acidity and continental glaciation are in some way intimately related and points to a teleconnection between Antarctica and the equatorial Pacific. The association between a decrease in ocean acidity and glaciation can be understood in terms of declining atmospheric carbon dioxide and low-resolution proxy records for Cenozoic pCO_2 change indicate significantly lower levels of pCO_2 for the Oligocene than for the Eocene (Pagani et al., 2005). However, no proxy pCO_2 data are yet available for the E–O transition itself.

Modeling studies suggest that an increase in deep-sea $[CO_3^{2-}]$ associated with a 1-km deepening of the CCD today yields a drawdown in atmospheric CO_2 of <25 ppmv (Sigman and Boyle, 2000; Zeebe and Westbroek, 2003). Nevertheless, the 100-ppm drawdown of atmospheric CO_2 at the Last Glacial Maximum (LGM) in the Pleistocene is associated with only a 100-m change in CCD, not a 4000-m change (Farrell and Prell, 1989), suggesting strong negative feedback and much less sensitive CCD response to atmospheric CO_2 change than simple models predict.

Antarctic glaciation may have triggered CCD deepening (Coxall et al., 2005) by a change in global ratio of $CaCO_3$ to C_{org} burial. In fact, the pronounced $\delta^{13}C$ increase seen in the E–O transition records suggest that the CCD deepened to compensate for increased C_{org} burial ratio relative to $CaCO_3$ (Coxall et al., 2005). However, the mechanism responsible for bringing about this change is a matter of debate. Coxall et al. (2005) reason that a simple mechanism to explain these events is shelf-to-basin $CaCO_3$ fractionation caused by glacioeustatic sea level fall associated with Antarctic glaciation. Rea and Lyle (2005) argue that the sea level fall associated with the glaciation (50 m, based on New Jersey margin records, e.g., Miller et al., 2005) is too small to have been the sole factor and invoke an increase in the delivery to the ocean of weathered Ca and HCO_3^- ions. **Olivarez Lyle and Lyle** (this volume, 2006) suggest that a temperature drop associated with the E/O may have increased C_{org} burial significantly by reducing the metabolic decomposition of organic matter before burial. Such a reduction in the dissolved inorganic carbon pool relative to weathered cations would also deepen the CCD. These (and other) competing hypotheses are now being tested using a range of modeling techniques.

Eocene

A chert-rich interval at roughly the early/middle Eocene boundary at all sites except Site 1215 (see Fig. **F2**) operationally divides Leg 199 Eocene studies into those of the Paleocene–early Eocene and those from the middle Eocene to the Eocene/Oligocene boundary. At Site 1215, the northernmost site of Leg 199, sedimentation switched from carbonates to red clay at ~52 Ma, in the early Eocene (Raffi et al., 2005), so studies of this site also fall within the Paleocene–early Eocene category. We discuss all the Paleocene–early Eocene work in the section on the Paleocene/Eocene boundary interval.

Synopsis of the Eocene

The Eocene is relatively poorly studied but Earth's climate is thought to have evolved from a transient warm burst (the PETM, at 55 Ma) to maximum Cenozoic warmth over a period of ~5 m.y. From that point

onward, Earth was on a cooling path, punctuated by significant rapid changes, such as that of the Eocene/Oligocene boundary (see Zachos et al., 2001, for a good overview). The paucity of high-resolution records in the Eocene has caused the impression that the Eocene was marked by only gradual change. More detailed records reveal significant numbers of transient warm and cold events lasting from a few hundred thousand years up to 2 m.y. (e.g., Bohaty and Zachos, 2003; Lourens et al., 2005; **Lyle et al.,** this volume).

Early Eocene

The early Eocene began with one of the most important Cenozoic transient events, the Paleocene/Eocene boundary event, or PETM (Zachos et al., 2001). The upper? Paleocene and lower Eocene sediments recovered during Leg 199 are marked by a very distinctive P/E boundary section (see Lyle, Wilson, Janecek, et al., 2002; Nomura et al., 2002; **Faul and Paytan,** this volume; **Knoop,** this volume; **Murphy et al.,** this volume; **Nomura and Takata,** this volume; **Nuñes and Norris,** this volume), with significant geochemical variations as well as the disappearance of carbonate that marks the PETM worldwide. The Paleocene and lower Eocene sediments are also distinguished by low numbers of radiolarians, unlike later Eocene intervals.

Within the Leg 199 transect, the lower Eocene has high carbonate, primarily reflecting the drilling strategy of the leg to sample shallow early Eocene sediment sections. The Eocene had a very shallow CCD, roughly 3200–3300 meters below sea level (mbsl), compared to a late Pleistocene equatorial Pacific CCD of ~4600 mbsl (Heath et al., 1977; Delaney and Boyle, 1988; Lyle, Wilson, Janecek, et al., 2002; Lyle, 2003; Rea and Lyle, 2005; **Lyle et al.,** this volume). The early Eocene transect was therefore drilled on ocean crust only slightly older than the P/E boundary to be near the shallow topography of the early Eocene rise crest (~2800 m). One interesting feature of the early Eocene is that carbonate was better preserved off the equator and not at the equator, opposite to all Neogene trends.

Early–Middle Eocene Transition

The early–middle Eocene transition, the warmest part of the Cenozoic, was poorly recovered at all Leg 199 sites because a significant numbers of chert horizons were found in this interval (Lyle, Wilson, Janecek, et al., 2002). During the leg there was significant speculation as to why the early/middle Eocene boundary was consistently chertified, but there has not yet been further study. Hypotheses that would explain extensive chert formation at the early/middle Eocene boundary range from the chemical to the kinetic, and the true explanation probably contains elements of many of the hypotheses. For example, biogenic opal sedimentation increased between the early and middle Eocene. Such a change in sediment composition may have initiated chert formation and the initial chert formation may have autocatalyzed further chertification. Because amorphous biogenic silica is converted to chert more rapidly in the presence of carbonate (Kastner et al., 1977), it may be significant that the chert interval lies just above the lower carbonates. Also, the conversion rate of biogenic opal to chert increases with temperature. It is probably more than coincidence that the warmest part of the Cenozoic, when bottom water temperatures exceeded 12°C, also has the highest development of cherts.

Middle and Late Eocene

Oxygen isotope values trend toward heavier values all through the middle and late Eocene, implying a long-term trend toward cooling conditions (Zachos et al., 2001). However, other paleoceanographic proxies show significantly more variability. Average rates of biogenic deposition in the equatorial Pacific are high between 50 and 40 Ma, or during the entire middle Eocene (Moore et al., 2004). Sedimentation rates dropped consistently throughout the late Eocene, with the latest Eocene occasionally being represented by a hiatus in off-equator sites along the Leg 199 transect (Lyle, Wilson, Janecek, et al., 2002). Carbonate accumulation events occurred roughly every 2.5 m.y. in the middle Eocene but switched to ~1-m.y. intervals after 37.5 Ma (**Lyle et al.,** this volume). The largest of the events (CAE-3, **Lyle et al.,** this volume) occurred between 42 and 40 Ma and was also a productivity event (**Olivarez Lyle and Lyle,** this volume). The CAE-3 interval is the only one in the middle and late Eocene to have significant numbers of diatoms in the radiolarian oozes, up to 50% of the total biogenic silica fraction near the end of CAE-3. **Steiger** (this volume) performed a preliminary study on the environmental changes in the CAE-3 interval from a radiolarian faunal analysis. He interprets the changes in radiolarian fauna to indicate cooling during the event. There clearly is additional information preserved in the fauna, but much of this information depends upon further studies to better determine the environments of specific radiolarian species.

Carbonate Compensation Depth

The Eocene/Oligocene boundary has long been recognized as the largest change of the CCD in the Cenozoic (van Andel et al., 1975; Heath et al., 1977; Delaney and Boyle, 1988; Rea and Lyle, 2005). However, until Leg 199 it was not recognized that the Eocene/Oligocene boundary also marked the change from a regime of high-amplitude CCD changes to one of relatively constant CCD. The equatorial Pacific CCD oscillated by several hundred meters a number of times during the Eocene (Rea and Lyle, 2005; **Lyle et al.,** this volume) but has only changed by 250 m or so throughout the Neogene (Lyle, 2003) and only by ~100 m in the Pleistocene (Farrell and Prell, 1989).

The major change of CCD at the Eocene/Oligocene boundary is attributed to the sudden lowering of sea level associated with the first continent-wide glaciation of Antarctica (Coxall et al., 2005). Yet, Rea and Lyle (2005) show that, assuming a sea level fall of ~50 m (Miller et al., 2005), the expansion of abyssal seafloor area available for carbonate deposition is significantly larger than the loss of shelf and shallow sea area by sea level lowering. The area of abyssal carbonate deposition expanded by ~25% of global Earth area, while lost shelf area occupied only 4% of global Earth area. Lyle et al. (unpubl. data) argue that the weathering flux of Ca and alkalinity must have increased rapidly by ~20% at the E/O boundary or that the dissolved inorganic carbon pool must have dropped dramatically.

A series of transient CCD events occurred in the Eocene (Lyle, Wilson, Janecek, et al., 2002; **Lyle et al.,** this volume). **Lyle et al.** (this volume) identified seven CCD events in the middle and late Eocene, demonstrated that high carbonate is associated with cooling, and showed that the largest event (CAE-3) ended because of carbon cycle changes. Such a change implies a large increase in atmospheric CO_2 associated with the shallowing of the CCD by more than 800 m and the

warming conditions. The large gyrations of the CCD in the Eocene imply that many stabilizing feedbacks of the Pleistocene and Holocene carbon cycle are missing in the Eocene.

Tripati et al. (2005a, 2005b) suggested that the CAE-3 cooling event was associated with 120 m of sea level change based upon comparison of oxygen isotopes (a combined ice volume and temperature signal) and Mg/Ca (controlled by temperature) in benthic foraminifers. This ice volume estimate is high in comparison to all available other lines of geological evidence, raising the possibility that the Mg/Ca temperature estimates are compromised. The CAE-3 transition is marked by major changes in carbonate dissolution, and strong dissolution artifacts are known to exist for the Mg/Ca paleothermometer (Lear et al., 2004). In addition, the basal section of sediments, just below the interval in question, contains euhedral diagenetic dolomite rendering these sediments of questionable reliability for paleothermometric study (Lyle, Wilson, Janecek, et al., 2002).

Independent evidence of sea level rise at the end of CAE-3 does not support the existence of a large ice cap. Seismic stratigraphy along the New Jersey margin suggests that the sea level rise at the end of CAE-3 was only ~30–50 m (Browning et al., 1996; Miller et al., 1998, 2005). The sheer volume of ice needed to cause a 120 m sea level drop is another important concern. Such an icecap is as large as the combined Northern and Southern Hemisphere ice caps at the LGM (21 ka), but evidence for extensive middle Eocene ice sheet development outside Antarctica does not exist. If the ice cap were confined to Antarctica, it would have to be double the thickness of the modern Antarctic ice cap under warmer conditions—a physical impossibility given the limits imposed on area by the Antarctic continent and strong dependence of ice sheet flow on stress (Coxall et al., 2005).

Paleoproductivity and Carbon Burial

Clearly, the biogeochemical cycles of the Eocene equatorial Pacific clearly were organized differently than the Holocene equatorial Pacific. One of the most impressive features of the middle and late Eocene are the presence of sugary radiolarian oozes that contain ~70% biogenic silica. Despite the high biogenic opal contents, there are almost no diatom tests (only a few percent, based on smear slides). In contrast, Holocene equatorial Pacific sediments contain 2 to 10 times as many diatoms as radiolarians (Lyle, Wilson, Janecek, et al., 2002). The Eocene thus has a short supply of larger phytoplankton characteristic of the modern equatorial Pacific. New estimates of opal deposition rate (Moore, 2005) suggest that the Eocene actually had relatively low MAR of opal compared to the Neogene.

The Eocene equatorial Pacific also has extremely low C_{org} contents and C_{org} MAR that are an order of magnitude below those of the Holocene or Pleistocene equatorial Pacific. **Olivarez Lyle and Lyle** (this volume, 2006) explored the implications of these low C_{org} contents and propose that the low C_{org} burial is caused by higher metabolic demand by marine ecosystems under high-temperature conditions. Such a metabolic demand in both marine and terrestrial ecosystems is an important feedback maintaining warm climate conditions.

Olivarez Lyle and Lyle (this volume, 2006) first compared C_{org} MAR to biogenic Ba MAR (a proxy for productivity) (Dymond et al., 1992) and determined that productivity in the Eocene equatorial Pacific was

not radically lower than the Holocene. Instead, low C_{org} was caused by much higher organic matter degradation before ultimate burial. After eliminating the possibility of much higher oxygen exposure times, the likely cause of such an increase in degradation is the temperature-dependence of heterotrophic metabolism. Metabolic respiration rates roughly double for a 10°C change in environmental temperature (Gillooly et al., 2001; Brown et al., 2004). Even though the amount of pelagic burial is small, changes in the net burial of C_{org} could significantly affect levels of atmospheric CO_2 on timescales of 10^4 years. In addition, the increase in organic matter degradation would affect the other shallow organic carbon reservoirs in soils and deltaic sediments, so that the feedback is probably stronger than a prediction based on pelagic sediments alone.

PALEOCENE/EOCENE BOUNDARY

One of the important objectives of Leg 199 was to investigate the structure of the Paleocene/Eocene boundary in the pelagic Pacific, to compare with other boundary sections worldwide. Such comparisons have now led to a hypothesis that deep circulation reversed at the P/E boundary during the PETM event (Nuñes and Norris, 2006).

P/E boundary sections were sampled at three of the Leg 199 drill sites (Sites 1215, 1220, and 1221; Lyle, Wilson, Janecek, et al., 2002), all of which are notable for high Mn contents, partly because all the sections were collected from basal sediment sections near ocean basement, where it is common to find deposition from mid-ocean-ridge hydrothermal plumes (Ruhlin and Owen, 1986; Lyle et al., 1987). Site 1215, at ~12°N when basement was formed, has >5% Mn in the basal section (**Knoop,** this volume) and Mn/Fe near the hydrothermal ratio for modern East Pacific Rise sediments (0.3) (Dymond, 1981). Site 1216 also shows evidence of enrichment with hydrothermal sediments in the lower sediment column (**Ito et al.,** this volume).

Sites 1220 and 1221, the two sites near the equator at the P/E boundary, show evidence for significant remobilization of Mn after deposition but no evidence that the Mn escapes the sediments. In the middle of a multicolored P/E boundary section at both Sites 1220 and 1221 there lies a black Mn oxide–rich sediment containing as much as 14.6% Mn and having Mn/Fe as high as 3.7 (Fig. **F10**) (Lyle, Wilson, Janecek, et al., 2002; **Knoop,** this volume). Such high Mn contents are similar to sediments from Guatemala Basin, which have high Mn inputs but are also subject to suboxic diagenesis (Finney et al., 1988). Under anoxic conditions, Mn is almost quantitatively removed from the sediments. The retention of high amounts of Mn oxide is strong evidence that the bottom waters and the uppermost sediments always contained oxygen. If bottom waters had become depleted in oxygen, the Mn oxides would not have been trapped.

There are other unusual but consistent geochemical signatures of the two P/E boundaries from Sites 1220 and 1221 (Lyle, Wilson, Janecek, et al., 2002; **Faul and Paytan,** this volume). Because the two sites are >200 km apart, the geochemical patterns must result from regional, not local, trends. Both P/E boundary intervals are marked by two high-Ba intervals, which **Faul and Paytan** (this volume) showed at Site 1221 to be primarily composed of barite.

Bains et al. (2000) previously reported high Ba in the P/E interval of two sites, one from the Blake Nose in the North Atlantic (Site 1051) and

F10. Digital images of the P/E boundary sediments, p. 37.

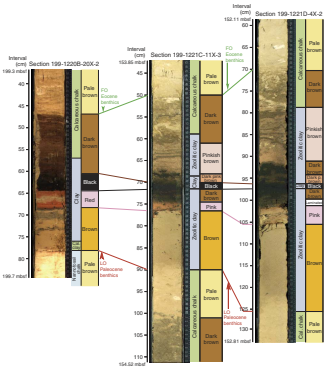

one from Maude Rise (Site 690) in the Atlantic sector of the Southern Ocean. They attributed the Ba peaks to paleoproductivity. **Faul and Paytan** (this volume) investigated Site 1221 and found that the Ba peaks consisted of barite and that the barite crystals resembled those derived from biogenic processes, not hydrothermal barite (observed near some marine hydrothermal vents). However, **Faul and Paytan** (this volume) and **Murphy et al.** (this volume) found that other elements associated with biogenic rain to the sediment were not as enriched as Ba. There was a P enrichment associated with the barite peaks (**Faul and Paytan,** this volume) but evidence of significant P loss from the sediments and more loss of P in the warmer conditions later in the boundary event. **Murphy et al.** (this volume) found no change in C_{org} or biogenic Si content across the Site 1221 P/E boundary on splits of samples from **Faul and Paytan** (this volume). **Murphy et al.** (this volume) attribute the difference between the C_{org} and Ba signal to metabolic burndown of the C_{org}.

Nuñes and Norris (this volume, 2006) investigated the change in stable isotope composition across the PETM at Sites 1220 and 1221 as well as 12 other P/E boundary sections around the world. From the distribution of carbon isotopes they hypothesize a switch from Southern Hemisphere deepwater sources to Northern Hemisphere sources during the excursion. Such a switch, if confirmed by further analyses in boundary sections, suggests an important way to quickly warm up the deep oceans. High-latitude northern sources of deep water were probably warmer than Antarctic sources, so provided a way to pump heat downward and provide a huge thermal reservoir to maintain global warmth.

The rapid change in both deepwater temperatures and global surface temperatures created terminal stresses for a variety of organisms—the largest benthic extinction of foraminifers in the Cenozoic is not associated with the Cretaceous/Tertiary boundary, for example, but with the PETM (Thomas, 2003). Large extinctions of marine plankton also mark the boundary. These ecological studies of the boundary sections from Leg 199 are only beginning, but important results are already surfacing. For example, **Nomura and Takata** (this volume) note that the extinction level of Paleocene benthic foraminifers is 30 cm below the carbon isotope excursion characteristic of the PETM, as found by **Nuñes and Norris** (this volume), suggesting that significant environmental changes led the postulated methane hydrate release that caused the carbon isotope event. The good P/E boundary section at Site 1215, combined with data from other P/E boundary intervals, allowed Raffi et al. (2005) to begin to explore the evolution of the calcareous nannoplankton from a biogeographic perspective. They find that some evolutionary events at the boundary are associated with the equatorial Atlantic, Tethys, and eastern Pacific (*Rhomboaster* spp.–*Discoaster araneus* association), some events appear global (loss of diversification of the genus *Fasciculithus*), while some are restricted to temperate latitudes (occurrence of *Zygrhablithus bijugatus*).

Leg 199 has clearly added important new P/E boundary sections to the growing global collection. The combined isotope, evolutionary, biogeographic, and paleoceanographic records are reaching a new level for which to understand this important global transient, and furthermore to get a better understanding of global Earth systems during extreme warmth.

SUMMARY

The Paleogene is a time of major change in global climate that holds critical information for understanding Earth system processes. The entire Paleogene was a period of extreme warmth when compared to modern climate conditions; the study of the Paleogene is thus pertinent to understand the processes that maintain warm Earth conditions.

ODP Leg 199 is the first drilling leg to study the Paleogene equatorial Pacific using modern scientific drilling technology. Study of the continuously recovered sections has been important for fundamental advances in Cenozoic chronostratigraphy and to understand Cenozoic motion of the Pacific plate. The first continuous sedimentary sections of Oligocene and middle–late Eocene age from the equatorial Pacific have been extremely important to understand major paleoceanographic events regionally as well as globally. Postcruise science from Leg 199 has developed precise timing of some of the first major Cenozoic glaciations and identification of transient, probably glacial, events within the Eocene.

Fundamental new information about global climate, the carbon cycle, and Cenozoic paleoproductivity has resulted from the study of Leg 199 sediments, but many new questions have appeared. What really is the relationship global warmth, weathering, and the carbon cycle? To what extent does global warmth regulate carbon burial? How can deep circulation reorganize itself in response to climate? Further work on Leg 199 sediments will help to answer these questions, especially when combined with further drilling that targets the Paleogene.

ACKNOWLEDGMENTS

We thank the captain and crew of the *JOIDES Resolution,* and our fellow scientific party, for making Leg 199 a success. This research used data provided by the Ocean Drilling Program (ODP). ODP is sponsored by the U.S. National Science Foundation (NSF) and participating countries under management of Joint Oceanographic Institutions (JOI), Inc. Funding for this research was also provided to Lyle by the U.S. Science Advisory Committee of ODP, NSF grants OCE-0240906 and OCE-0451291 and to Wilson by NERC UK IODP grant NER/T/S/2002/00400 and NERC NER/A/S/2003/00377.

REFERENCES

Bains, S., Norris, R.D., Corfield, R.M., and Faul, K.L., 2000. Termination of global warmth at the Palaeocene–Eocene boundary through productivity feedback. *Nature (London, U. K.),* 407(6801):171–174. **doi:10.1038/35025035**

Barker, P.F., 2001. Scotia Sea regional tectonic evolution: implications for mantle flow and palaeocirculation. *Earth Sci. Rev.,* 55(1–2):1–39. **doi:10.1016/S0012-8252(01)00055-1**

Bloomer, S.F., Mayer, L.A., and Moore, T.C., Jr., 1995. Seismic stratigraphy of the eastern equatorial Pacific Ocean: Paleoceanographic implications. *In* Pisias, N.G., Mayer, L.A., Janecek, T.R., Palmer-Julson, A., and van Andel, T.H. (Eds.), *Proc. ODP, Sci. Results,* 138: College Station, TX (Ocean Drilling Program), 537–553.

Bohaty, S.M., and Zachos, J.C., 2003. Significant Southern Ocean warming event in the late middle Eocene. *Geology,* 31(11):1017–1020. **doi:10.1130/G19800.1**

Brown, J.H., Gillooly, J.F., Allen, A.P., Savage, V.M., and West, G.B., 2004. Toward a metabolic theory of ecology. *Ecology,* 85(7):1771–1789.

Browning, J.V., Miller, K.G., and Pak, D.K., 1996. Global implications of lower to middle Eocene sequence boundaries on the New Jersey Coastal Plain—the Icehouse cometh. *Geology,* 24(7):639–642. **doi:10.1130/0091-7613(1996)024<0639:GIOLTM>2.3.CO;2**

Cande, S.C., and Kent, D.V., 1992. A new geomagnetic polarity time scale for the Late Cretaceous and Cenozoic. *J. Geophys. Res.,* 97(10):13917–13951.

Cande, S.C., and Kent, D.V., 1995. Revised calibration of the geomagnetic polarity timescale for the Late Cretaceous and Cenozoic. *J. Geophys. Res.,* 100(B4):6093–6095. **doi:10.1029/94JB03098**

Chase, C.G., Gregory-Wodzicki, K.M., Parrish, J.T., and Decelles, P.G., 1998. Topographic history of the western cordillera of North America and controls on climate. *In* Crowley, T.J., and Burke, K.C., (Eds.), *Tectonic Boundary Conditions for Climate Reconstruction:* New York (Oxford Univ. Press), 73–100.

Chavez, F.P., and Barber, R.T., 1987. An estimate of new production in the equatorial Pacific. *Deep-Sea Res., Part A,* 34(7):1229–1243. **doi:10.1016/0198-0149(87)90073-2**

Chavez, F.P., Buck, K.R., Service, S.K., Newton, J., and Barber, R.T., 1996. Phytoplankton variability in the central and eastern tropical Pacific. *Deep Sea Res., Part II,* 43(4–6):835–870. **doi:10.1016/0967-0645(96)00028-8**

Chavez, F.P., Strutton, P.G., Friederich, G.E., Feely, R.A., Feldman, G.C., Foley, D.G., and McPhaden, M.J., 1999. Biological and chemical response of the Equatorial Pacific Ocean to the 1997–1998 El Niño. *Science,* 286(5447):2126–2131. **doi:10.1126/science.286.5447.2126**

Coates, A.G., and Obando, J.A., 1996. The geologic evolution of the Central American Isthmus. *In* Jackson, J.B.C., Budd, A.F., and Coates, A.G. (Eds.), *Evolution and Environment in Tropical America:* Chicago (Univ. of Chicago Press), 21–55.

Coxall, H.K., Wilson, P.A., Pälike, H., Lear, C.H., and Backman, J., 2005. Rapid stepwise onset of Antarctic glaciation and deeper calcite compensation in the Pacific Ocean. *Nature (London, U. K.),* 433(7021):53–57. **doi:10.1038/nature03135**

DeConto, R.M., and Pollard, D., 2003. Rapid Cenozoic glaciation of Antarctica induced by declining atmospheric CO_2. *Nature (London, U. K.),* 421(6920):245–249. **doi:10.1038/nature01290**

Delaney, M.L., and Boyle, E.A., 1988. Tertiary paleoceanic chemical variability: unintended consequences of simple geochemical models. *Paleoceanography,* 3:137–156.

Demicco, R.V., Lowenstein, T.K., and Hardie, L.A., 2003. Atmospheric pCO_2 since 60 Ma from records of seawater pH, calcium, and primary carbonate mineralogy. *Geology,* 31(9):793–796. **doi:10.1130/G19727.1**

Dickens, G.R., O'Neil, J.R., Rea, D.K., and Owen, R.M., 1995. Dissociation of oceanic methane hydrate as a cause of the carbon isotope excursion at the end of the Paleocene. *Paleoceanography,* 10(6):965–972. **doi:10.1029/95PA02087**

Diester-Haass, L., and Zahn, R., 2001. Paleoproductivity increase at the Eocene–Oligocene climatic transition: ODP/DSDP Sites 763 and 592. *Palaeogeogr., Palaeoclimatol., Palaeoecol.,* 172(1–2):153–170. **doi:10.1016/S0031-0182(01)00280-2**

Dymond, J., 1981. Geochemistry of Nazca plate surface sediments: an evaluation of hydrothermal, biogenic, detrital, and hydrogenous sources. *In* Kulm, L.D., Dymond, J., Dasch, E.J., Hussong, D.M., and Roderick, R. (Eds.), *Nazca Plate: Crustal Formation and Andean Convergence*. Mem.—Geol. Soc. Am., 154:133–173.

Dymond, J., Suess, E., and Lyle, M., 1992. Barium in deep-sea sediment: a geochemical proxy for paleoproductivity. *Paleoceanography,* 7:163–181.

Farrell, J.W., and Prell, W.L., 1989. Climatic change and $CaCO_3$ preservation: an 800,000 year bathymetric reconstruction from the central equatorial Pacific Ocean. *Paleoceanography,* 4(4):447–466.

Finney, B.P., Lyle, M.W., and Heath, G.R., 1988. Sedimentation at MANOP Site H (eastern equatorial Pacific) over the past 400,000 years: climatically induced redox variations and their effects on transition metal cycling. *Paleoceanography,* 3:169–189.

Funakawa, S., Nishi, H., Moore, T.C., and Nigrini, C.A., 2006. Radiolarian faunal turnover and paleoceanographic change around Eocene/Oligocene boundary in the central equatorial Pacific, ODP Leg 199, Holes 1218A, 1219A, and 1220A. *Palaeogeogr., Palaeoclimatol., Palaeoecol.,* 230(3–4):183–203. **doi:10.1016/j.palaeo.2005.07.014**

Gillooly, J.F., Brown, J.H. West, G.B., Savage, V.M., and Charnov, E.L., 2001. Effects of size and temperature on metabolic rate. *Science,* 293(5538):2248–2251. **doi:10.1126/science.1061967**

Grimes, S.T., Hooker, J.J., Collinson, M.E., and Mattey, D.P., 2005. Summer temperatures of late Eocene to early Oligocene freshwaters. *Geology,* 33(3):189–192. **doi:10.1130/G21019.1**

Harrison, T.M., Yin, A., and Ryrson, F., 1998. Orographic evolution of the Himalaya and Tibetan Plateau. *In* Crowley, T.J., and Burke, K.C. (Eds.), *Tectonic Boundary Conditions for Climate Reconstructions*. Oxford Monogr. Geol. Geophys., 39:39–72.

Heath, G.R., Moore, T.C., Jr., and van Andel, T.H., 1977. Carbonate accumulation and dissolution in the equatorial Pacific during the past 45 million years. *In* Andersen, N.R., and Malahoff, A. (Eds.), *The Fate of Fossil Fuel CO_2 in the Oceans:* New York (Plenum), 627–639.

Honjo, S., Dymond, J., Collier, R., and Manganini, S.J., 1995. Export production of particles to the interior of the equatorial Pacific Ocean during the 1992 EqPac experiment. *Deep-Sea Res., Part II,* 42(2–3):831–870. **doi:10.1016/0967-0645(95)00034-N**

Huber, M., 2002. Straw man 1: a preliminary view of the tropical Pacific from a global coupled climate model simulation of the early Paleogene. *In* Lyle, M., Wilson, P.A., Janecek, T.R., et al., *Proc. ODP, Init. Repts.,* 199, 1–30 [CD-ROM]. Available from: Ocean Drilling Program, Texas A&M University, College Station TX 77845-9547, USA. [**HTML**]

Huber, M., Brinkhuis, H., Stickley, C.E., Döös, K., Sluijs, A., Warnaar, J., Schellenberg, S.A., and Williams, G.L., 2004. Eocene circulation of the Southern Ocean: was Antarctica kept warm by subtropical waters? *Paleoceanography,* 19(4):PA4026. **doi:10.1029/2004PA001014**

Huber, M., and Caballero, R., 2003. Eocene El Niño: evidence for robust tropical dynamics in the "hothouse." *Science,* 299(5608):877–881. **doi:10.1126/science.1078766**

Huber, M., and Nof, D., 2006. The ocean circulation in the southern hemisphere and its climatic impacts in the Eocene. *Palaeogeogr., Palaeoclimatol., Palaeoecol.,* 231(1–2):9–28. **doi:10.1016/j.palaeo.2005.07.037**

Huber, M., and Sloan, L.C., 1999. Warm climate transitions: a general circulation modeling study of the Late Paleocene Thermal Maximum (~56 Ma). *J. Geophys. Res.,* 104(D14):16633–16656. **doi:10.1029/1999JD900272**

Huber, M., and Sloan, L.C., 2001. Heat transport, deep waters, and thermal gradients: coupled simulation of an Eocene greenhouse climate. *Geophys. Res. Lett.,* 28(18):3481–3484. **doi:10.1029/2001GL012943**

Huber, M., Sloan, L.C., and Shellito, C., 2003. Early Paleogene oceans and climate: a fully coupled modeling approach using the NCAR CCSM. *In* Wing, S.L., Gingerich, P.D., Schmitz, B., and Thomas, E. (Eds.), *Causes and Consequences of Globally Warm Climates in the Early Paleogene*. Spec. Pap.—Geol. Soc. Am., 369:25–47.

Kastner, M., Keene, J.B., and Gieskes, J.M., 1977. Diagenesis of siliceous oozes, I. Chemical controls on the rate of opal-A to opal-CT transformation—an experimental study. *Geochim. Cosmochim. Acta,* 41(8):1041–1051. **doi:10.1016/0016-7037(77)90099-0**

Kennett, J.P., Keller, G., and Srinivasan, M.S., 1985. Miocene planktonic foraminiferal biogeography and paleoceanographic development of the Indo-Pacific region. *In* Kennett, J.P. (Ed.), *The Miocene Ocean: Paleoceanography and Biogeography*. Mem.—Geol. Soc. Am., 163:197–236.

Kennett, J.P., and Stott, L.D., 1991. Abrupt deep-sea warming, paleoceanographic changes and benthic extinctions at the end of the Palaeocene. *Nature (London, U. K.),* 353(6341):225–229. **doi:10.1038/353225a0**

Kohn, M.J., Josef, J.A., Madden, R., Kay, R., Vucetich, G., and Carlini, A.A., 2004. Climate stability across the Eocene–Oligocene transition, southern Argentina. *Geology,* 32(7):621–624. **doi:10.1130/G20442.1**

Lanci, L., Parés, J.M., Channell, J.E.T., and Kent, D.V., 2004. Miocene magnetostratigraphy from equatorial Pacific sediments (ODP Site 1218, Leg 199). *Earth Planet. Sci. Lett.,* 226(1–2):207–224. **doi:10.1016/j.epsl.2004.07.025**

Lanci, L., Parés, J.M., Channell, J.E.T., and Kent, D.V., 2005. Oligocene magnetostratigraphy from equatorial Pacific sediments (ODP Sites 1218 and 1219, Leg 199). *Earth Planet. Sci. Lett.,* 237(3–4):617–634. **doi:10.1016/j.epsl.2005.07.004**

Laskar, J., Joutel, F., and Boudin, F., 1993. Orbital, precessional, and insolation quantities for the Earth from –20 Myr to +10 Myr. *Astron. Astrophys.,* 270:522–533.

Laskar, J., Robutel, P., Joutel, F., Gastineau, M., Correia, A.C.M., and Levrard, B., 2004. A long-term numerical solution for the insolation quantities of the Earth. *Astron. Astrophys.,* 428(1):261–285. **doi:10.1051/0004-6361:20041335**

Latimer, J.C., and Filippelli, G.M., 2002. Eocene to Miocene terrigenous inputs and export production: geochemical evidence from ODP Leg 177, Site 1090. *Palaeogeogr., Palaeoclimatol., Palaeoecol.,* 182(3–4):151–164. **doi:10.1016/S0031-0182(01)00493-X**

Lawver, L.A., and Gahagan, L.M., 1998. Opening of Drake Passage and its impact on Cenozoic ocean circulation. *In* Crowley, T.J., and Burke, K.C. (Eds.), *Tectonic Boundary Conditions for Climate Reconstructions*. Oxford Monogr. Geol. Geophys., 39:212–223.

Lawver, L.A., and Gahagan, L.M., 2003. Evolution of Cenozoic seaways in the circum-Antarctic region. *Palaeogeogr., Palaeoclimatol., Palaeoecol.,* 198(1–2):11–37. **doi:10.1016/S0031-0182(03)00392-4**

Lear, C.H., Elderfield, H., and Wilson, P.A., 2000. Cenozoic deep-sea temperatures and global ice volumes from Mg/Ca in benthic foraminiferal calcite. *Science,* 287:269–272.

Lear, C.H., Rosenthal, Y., Coxall, H.K., and Wilson, P.A., 2004. Late Eocene to early Miocene ice-sheet dynamics and the global carbon cycle. *Paleoceanography,* 19(4):PA4015. **doi:10.1029/2004PA001039**

Livermore, R., Nankivell, A., Eagles, G., and Morris, P., 2005. Paleogene opening of Drake Passage. *Earth Planet. Sci. Lett.,* 236(1–2):459–470. **doi:10.1016/j.epsl.2005.03.027**

Lyle, M., 2003. Neogene carbonate burial in the Pacific Ocean. *Paleoceanography,* 18(3):1059. **doi:10.1029/2002PA000777**

Lyle, M., Leinen, M., Owen, R.M., and Rea, D.K., 1987. Late Tertiary history of hydrothermal deposition at the East Pacific Rise: correlation to volcano-tectonic events. *Geophys. Res. Lett.,* 14:595–598.

Lyle, M., Liberty, L., Moore, Jr., T.C., and Rea, D.K., 2002. Development of a seismic stratigraphy for the Paleogene sedimentary section, central tropical Pacific Ocean. *In* Lyle, M., Wilson, P.A., Janecek, T.R., et al., *Proc. ODP, Init. Repts.,* 199, 1–22 [Online]. Available from World Wide Web: <**http://www-odp.tamu.edu/publications/199_IR/VOLUME/CHAPTERS/IR199_04.PDF**>.

Lyle, M., Wilson, P.A., Janecek, T.R., et al., 2002. *Proc. ODP, Init. Repts.,* 199 [Online]. Available from World Wide Web: <**http://www-odp.tamu.edu/publications/199_IR/199ir.htm**>.

Mayer, L.A., 1991. Extraction of high-resolution carbonate data for palaeoclimate reconstruction. *Nature (London, U. K.),* 352(6331):148–150. **doi:10.1038/352148a0**

Mayer, L.A., Shipley, T.H., Theyer, F., Wilkens, R.H., and Winterer, E.L., 1985. Seismic modeling and paleoceanography at Deep Sea Drilling Project Site 574. *In* Mayer, L., Theyer, F., Thomas, E., et al., *Init. Repts. DSDP,* 85: Washington (U.S. Govt. Printing Office), 947–970.

Mayer, L.A., Shipley, T.H., and Winterer, E.L., 1986. Equatorial Pacific seismic reflectors as indicators of global oceanographic events. *Science,* 233:761–764.

Miller, K., Fairbanks, R., and Mountain, G., 1987. Tertiary oxygen isotope synthesis, sea level history, and continental margin erosion. *Paleoceanography,* 2:1–19.

Miller, K.G., Feigenson, M.D., Kent, D.V., and Olsson, R.K., 1988. Upper Eocene to Oligocene isotope ($^{87}Sr/^{86}Sr$, $\delta^{18}O$, $\delta^{13}C$) standard section, Deep Sea Drilling Project Site 522. *Paleoceanography,* 3:223–233.

Miller, K.G., Kent, D.V., Brower, A.N., Bybell, L.M., Feigenson, M.D., Olsson, R.K., and Poore, R.Z., 1990. Eocene–Oligocene sea-level changes on the New Jersey coastal plain linked to the deep-sea record. *Geol. Soc. Am. Bull.,* 102:331–339.

Miller, K.G., Kominz, M.A., Browning, J.V., Wright, J.D., Mountain, G.S., Katz, M.E., Sugarman, P.J., Cramer, B.S., Christie-Blick, N., and Pekar, S.F., 2005. The Phanerozoic record of global sea-level change. *Science,* 310(5752):1293–1298. **doi:10.1126/science.1116412**

Miller, K.G., Liu, C., and Feigenson, M.D., 1996. Oligocene to middle Miocene Sr-isotopic stratigraphy of the New Jersey continental slope. *In* Mountain, G.S., Miller, K.G., Blum, P., Poag, C.W., and Twichell, D.C. (Eds.), *Proc. ODP, Sci. Results,* 150: College Station, TX (Ocean Drilling Program), 97–114.

Miller, K.G., Mountain, G.S., Browning, J.V., Kominz, M., Sugarman, P.J., Christie-Blick, N., Katz, M.E., and Wright, J.D., 1998. Cenozoic global sea level, sequences, and the New Jersey transect: results from coastal plain and continental slope drilling. *Rev. Geophys.,* 36:569–601.

Miller, K.G., Thompson, P.R., and Kent, D.V., 1993. Integrated late Eocene–Oligocene stratigraphy of the Alabama coastal plain: correlation of hiatuses and stratal surfaces to glacioeustatic lowerings. *Paleoceanography,* 8:313–331.

Miller, K.G., Wright, J.D., and Fairbanks, R.G., 1991. Unlocking the Ice House: Oligocene–Miocene oxygen isotopes, eustasy, and margin erosion. *J. Geophys. Res.,* 96:6829–6848.

Mitchell, N.C., and Lyle, M.W., 2005. Patchy deposits of Cenozoic pelagic sediments in the central Pacific. *Geology,* 33(1):49–52. **doi:10.1130/G21134.1**

Moore, T.C., 2005. Opal accumulation in the equatorial Pacific. *Eos, Trans. Am. Geophys. Union,* 86(52)(Suppl.):PP24A-05. (Abstract)

Moore, T.C., Jr., Backman, J., Raffi, I., Nigrini, C., Sanfilippo, A., Pälike, H., and Lyle, M., 2004. Paleogene tropical Pacific: clues to circulation, productivity, and plate motion. *Paleoceanography,* 19(3):PA3013. **doi:10.1029/2003PA000998**

Murray, R.W., Leinen, M., and Isern, A.R., 1993. Biogenic flux of Al to sediment in the central equatorial Pacific Ocean: evidence for increased productivity during glacial periods. *Paleoceanography,* 8:651–670.

Nomura, R., Nishi, H., and Leg 199 Shipboard Party, L.S., 2002. Lithological changes across the Paleocene/Eocene boundary. *Chishitsugaku Zasshi,* 108(10):17–18.

Norris, R.D., and Röhl, U., 1999. Carbon cycling and chronology of climate warming during the Palaeocene/Eocene transition. *Nature (London, U. K.),* 401(6755):775–778. **doi:10.1038/44545**

Nuñes, F., and Norris, R.D., 2006. Abrupt reversal in ocean overturning during the Palaeocene/Eocene warm period. *Nature (London, U. K.),* 439(7072):60–63. **doi:10.1038/nature04386**

Olivarez Lyle, A., and Lyle, M.W., 2006. Missing organic carbon in Eocene marine sediments: is metabolism the biological feedback that maintains end-member climates? *Paleoceanography,* 21(2):PA2007. **doi:10.1029/2005PA001230**

Pagani, M., Arthur, M.A., and Freeman, K.H., 1999. Miocene evolution of atmospheric carbon dioxide. *Paleoceanography,* 14(3):273–292. **doi:10.1029/1999PA900006**

Pagani, M., Zachos, J.C., Freeman, K.H., Tipple, B., and Bohaty, S., 2005. Marked decline in atmospheric carbon dioxide concentrations during the Paleogene. *Science,* 309(5734):600–603. **doi:10.1126/science.1110063**

Pälike, H., Laskar, J., and Shackleton, N.J., 2004. Geological constraints of the chaotic diffusion of the Solar System. *Geology,* 32(11)929–932. **doi:10.1130/G20750.1**

Parés, J.M., and Lanci, L., 2004. A complete middle Eocene–early Miocene magnetic polarity stratigraphy in equatorial Pacific sediments (ODP Site 1220). *In* Channell, J.E.T., Kent, D.V., Lowrie, W., and Meert, J. (Eds.), *Timescales of the Paleomagnetic Field*. Geophys. Monogr., 145:131–140.

Parés, J.M., and Moore, T.C., 2005. New evidence for Hawaiian hotspot plume motion since the Eocene. *Earth Planet. Sci. Lett.,* 237(3–4):951–959. **doi:10.1016/j.epsl.2005.06.012**

Pearson, P.N., and Palmer, M.R., 2000. Atmospheric carbon dioxide concentrations over the past 60 million years. *Nature (London, U. K.),* 406(6979):695–699. **doi:10.1038/35021000**

Pekar, S.F., Christie-Blick, N., Kominz, M.A., and Miller, K.G., 2002. Calibration between eustatic estimates from backstripping and oxygen isotopic records for the Oligocene. *Geology,* 30(10):903–906. **doi:10.1130/0091-7613(2002)030<0903:CBEEFB>2.0.CO;2**

Pfuhl, H.A., and McCave, I.N., 2005. Evidence for late Oligocene establishment of the Antarctic circumpolar current. *Earth Planet. Sci. Lett.,* 235(3–4):715–728. **doi:10.1016/j.epsl.2005.04.025**

Raffi, I., Backman, J., and Pälike, H., 2005. Changes in calcareous nannofossil assemblages across the Paleocene/Eocene transition from the paleo-equatorial Pacific Ocean. *Palaeogeogr., Palaeoclimatol., Palaeoecol.,* 226(1–2):93–126. **doi:10.1016/j.palaeo.2005.05.006**

Rea, D.K., and Lyle, M.W., 2005. Paleogene calcite compensation depth in the eastern subtropical Pacific: answers and questions. *Paleoceanography,* 20(1):PA1012. **doi:10.1029/2004PA001064**

Royer, D., 2002. Estimating latest Cretaceous and Tertiary atmospheric CO_2 concentration from stomatal indices [Ph.D. thesis]. Yale Univ., New Haven, CT.

Royer, D.L., Berner, R.A., Montanez, I.P, Tabor, N.J., and Beerling, D.J., 2004. CO_2 as a primary driver of Phanerozoic climate. *GSA Today,* 14(3):4–10.

Ruhlin, D.E., and Owen, R.M., 1986. The rare earth element geochemistry of hydrothermal sediments from the East Pacific Rise: examination of a seawater scavenging mechanism. *Geochim. Cosmochim. Acta,* 50(3):393–400. **doi:10.1016/0016-7037(86)90192-4**

Sanfilippo, A., and Nigrini, C., 1998. Code numbers for Cenozoic low latitude radiolarian biostratigraphic zones and GPTS conversion tables. *Mar. Micropaleontol.,* 33(1-2):109–117. **doi:10.1016/S0377-8398(97)00030-3**

Scher, H.D., and Martin, E.E., 2006. Timing and climatic consequences of the opening of Drake Passage. *Science,* 312(5772):428–430. **doi:10.1126/science.1120044**

Shackleton, N.J., 1986. Paleogene stable isotope events. *Palaeogeogr., Palaeoclimatol., Palaeoecol.,* 57(1):91–102. **doi:10.1016/0031-0182(86)90008-8**

Shackleton, N.J., and Kennett, J.P., 1975. Paleotemperature history of the Cenozoic and the initiation of Antarctic glaciation: oxygen and carbon isotope analyses in DSDP Sites 277, 279, and 281. *In* Kennett, J.P., Houtz, R.E., et al., *Init. Repts. DSDP,* 29: Washington (U.S. Govt. Printing Office), 743–755.

Shipboard Scientific Party, 2002. Leg 199 summary. *In* Lyle, M., Wilson, P.A., Janecek, T.R., et al., *Proc. ODP, Init. Repts.,* 199: College Station TX (Ocean Drilling Program), 1–87. [**HTML**]

Sigman, D.M., and Boyle, E.A., 2000. Glacial/interglacial variations in atmospheric carbon dioxide. *Nature (London, U. K.),* 407(6806):859–869. **doi:10.1038/35038000**

Stickley, C.E., Brinkhuis, H., Schellenberg, S.A., Sluijs, A., Röhl, U., Fuller, M., Grauert, M., Huber, M., Warnaar, J., and Williams, G.L., 2004. Timing and nature of the deepening of the Tasmanian Gateway. *Paleoceanography,* 19(4):PA4027. **doi:10.1029/2004PA001022**

Tarduno, J.A., Duncan, R.A., Scholl, D.W., Cottrell, R.D., Steinberger, B., Thordarson, T., Kerr, B.C., Neal, C.R., Frey, F.A., Torii, M., and Carvallo, C., 2003. The Emperor Seamounts: southward motion of the Hawaiian hotspot plume in Earth's mantle. *Science,* 301(5636):1064–1069. **doi:10.1126/science.1086442**

Thomas, D.J., Bralower, T.J., and Jones, C.E., 2003. Neodymium isotopic reconstruction of late Paleocene–early Eocene thermohaline circulation. *Earth Planet. Sci. Lett.,* 209(3–4):309–322. **doi:10.1016/S0012-821X(03)00096-7**

Thomas, E., 2003. Extinction and food on the seafloor: a high-resolution benthic foraminiferal record across the initial Eocene thermal maximum, Southern Ocean Site 690. *In* Wing, S.L., Gingerich, P.D., Schmitz, B., and Thomas, E. (Eds.), *Causes and Consequences of Globally Warm Climates in the Early Paleogene,* Spec. Pap.—Geol. Soc. Am., 369:319–332.

Tripati, A., Backman, J., Elderfield, H., and Ferretti, P., 2005a. Eocene bipolar glaciation associated with global carbon cycle changes. *Nature (London, U. K.),* 436:341–346. **doi:10.1038/nature03874**

Tripati, A., Backman, J., Elderfield, H., and Ferretti, P., 2005b. Corrigendum: Eocene bipolar glaciation associated with global carbon cycle changes. *Nature (London, U. K.),* 438(7064):122. **doi:10.1038/nature04289**

van Andel, T.H., Heath, G.R., and Moore, T.C., Jr., 1975. *Cenozoic History and Paleoceanography of the Central Equatorial Pacific Ocean: A Regional Synthesis of Deep Sea Drilling Project Data.* Mem.—Geol. Soc. Am., 143.

Vanden Berg, M.D., and Jarrard, R.D, 2002. Determination of equatorial Pacific mineralogy using light absorption spectroscopy. *In* Lyle, M.W., Wilson, P.A., Janecek, T.R., et al., *Proc. ODP, Init. Repts.,* 199, 1–20 [CD-ROM]. Available from: Ocean Drilling Program, Texas A&M University, College Station TX 77845-9547, USA. [**HTML**]

Vanden Berg, M.D., and Jarrard, R.D., 2004. Cenozoic mass accumulation rates in the equatorial Pacific based on high-resolution mineralogy of Ocean Drilling Program Leg 199. *Paleoceanography,* 19(2):PA2021. **doi:10.1029/2003PA000928**

Wade, B.S., and Pälike, H., 2004. Oligocene climate dynamics. *Paleoceanography,* 19(4):PA4019. **doi:10.1029/2004PA001042**

Wyrtki, K., 1981. An estimate of equatorial upwelling in the Pacific. *J. Phys. Oceanogr.,* 11(9):1205–1214. **doi:10.1175/1520-0485(1981)011<1205:AEOEUI>2.0.CO;2**

Zachos, J., Pagani, M., Sloan, L., Thomas, E., and Billups, K., 2001. Trends, rhythms, and aberrations in global climate 65 Ma to present. *Science,* 292(5517):686–693. **doi:10.1126/science.1059412**

Zachos, J.C., Rea, D.K., Seto, K., Niitsuma, N., and Nomura, R., 1992. Paleogene and early Neogene deep water history of the Indian Ocean: inferences from stable isotopic records. *In* Duncan, R.A., Rea, D.K., Kidd, R.B., von Rad, U., and Weissel, J.K. (Eds.), *Synthesis of Results from Scientific Drilling in the Indian Ocean.* Geophys. Monogr., 70:351–386.

Zachos, J.C., Röhl, U., Schellenberg, S.A., Sluijs, A., Hodell, D.A., Kelly, D.C., Thomas, E., Nicolo, M., Raffi, I., Lourens, L.J., McCarren, H., and Kroon, D., 2005. Rapid acidification of the ocean during the Paleocene–Eocene Thermal Maximum. *Science,* 308(5728):1611–1615. **doi:10.1126/science.1109004**

Zachos, J.C., Wara, M.W., Bohaty, S., Delaney, M.L., Petrizzo, M.R., Brill, A., Bralower, T.J., and Premoli-Silva, I., 2003. A transient rise in tropical sea surface temperature during the Paleocene–Eocene Thermal Maximum. *Science,* 302(5650):1551–1554. **doi:10.1126/science.1090110**

Zeebe, R.E., and Westbroek, P., 2003. A simple model for the $CaCO_3$ saturation state of the ocean: the "Strangelove," the "Neritan," and the "Cretan" Ocean. *Geochem., Geophys., Geosyst.,* 4(12):1104. **doi:10.1029/2003GC000538**

Figure F1. Circulation and upwelling from a coupled ocean-atmosphere general circulation model (from Huber, 2002). Streamlines represent circulation at a depth of ~100 m. Whereas there are strong similarities to modern ocean circulation, there are important differences. Most notably, there is a southern Pacific subpolar gyre to complement the Alaska Gyre in the North Pacific and there is one southern subtropical gyre that sweeps through both the South Pacific and Indian Oceans. The Alaska Gyre is also shifted northward by 10° when compared to its modern position. Red = regions of vigorous upwelling; green to blue = regions of weak upwelling; white = areas of mean downwelling.

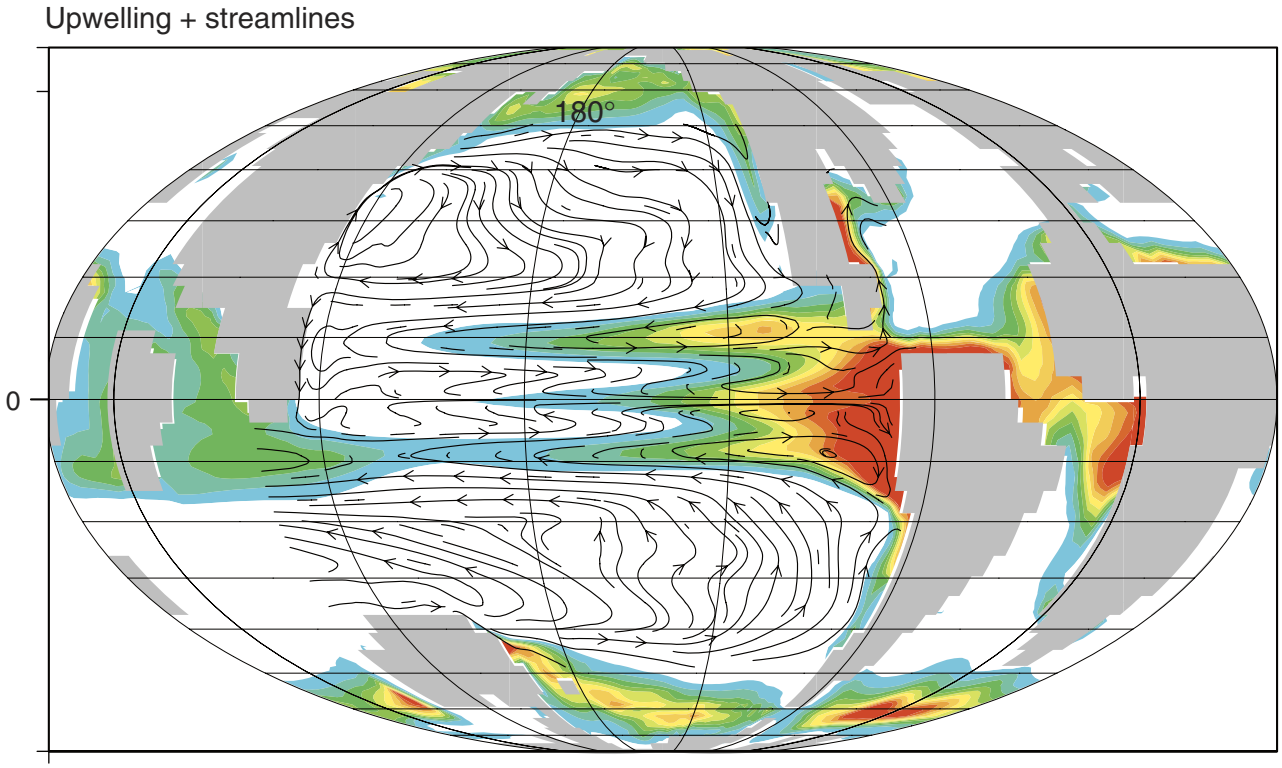

Figure F2. Lithologic summary of Leg 199 drilling showing lithostratigraphic units in the equatorial Pacific (from Shipboard Scientific Party, 2002). O/M = Oligocene/Miocene boundary, E/O = Eocene/Oligocene boundary, P/E = Paleocene/Eocene boundary, RN = Neogene radiolarian zone, RP = Paleogene radiolarian zone, NP = Paleogene nannofossil zone. Unit 1 (brown) is a surficial clay with varying amounts of radiolarians. Unit 2 (light blue) is Oligocene–lower Miocene nannofossil ooze/chalk. Unit 3 (light green) is middle–upper Eocene radiolarian ooze and clay. Unit 4 (white) is a chert-rich unit of middle–lower Eocene age. Unit 5 (pink) is lower Eocene nannofossil chalk.

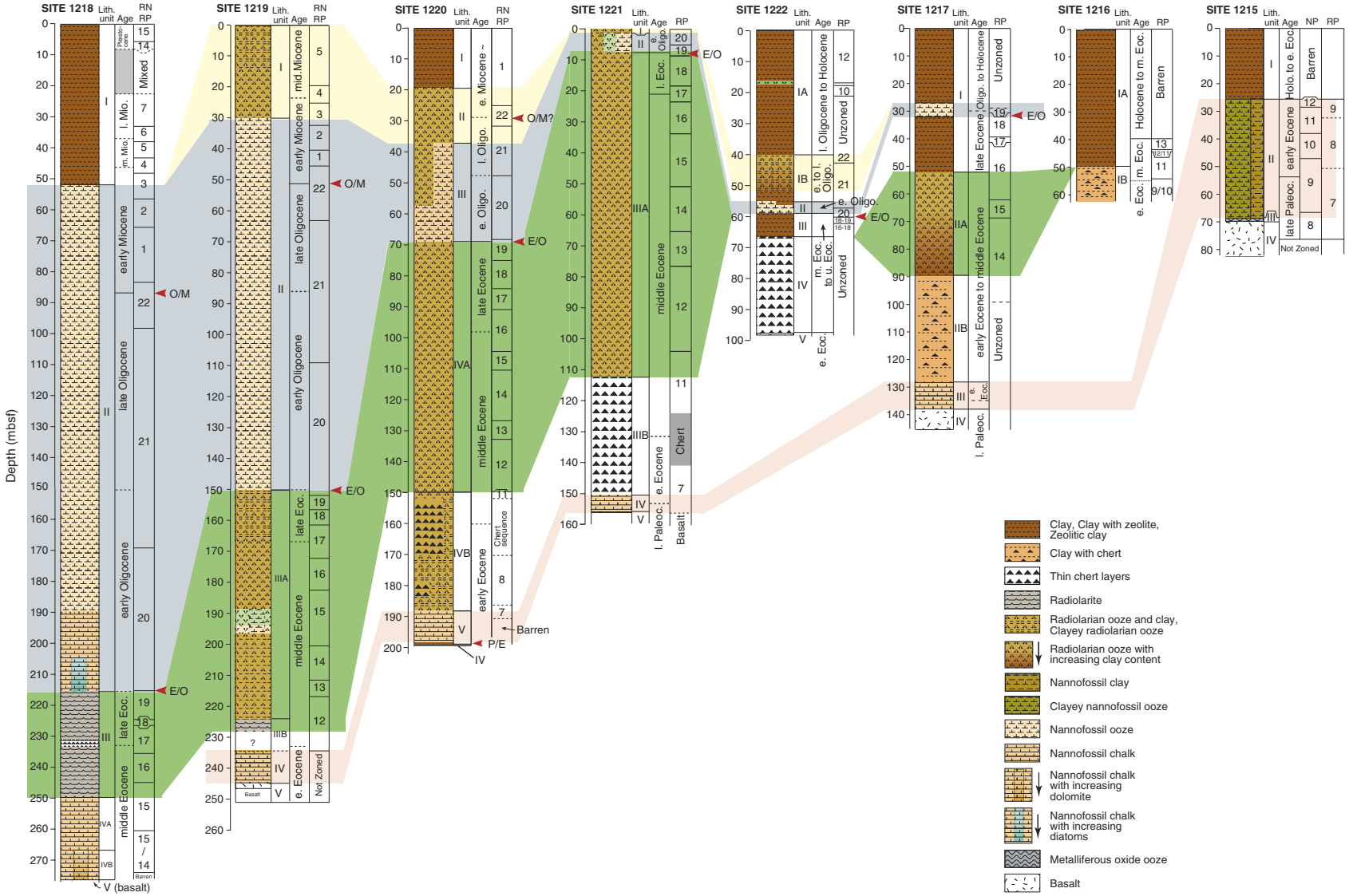

Figure F3. Map of the central tropical Pacific showing (**A**) Leg 199 drill sites and Deep Sea Drilling Project (DSDP) drill sites on regional bathymetry, and (**B**) Leg 199 drill sites superimposed on the approximate position of magnetic Anomaly An25n (58.9–56.4 Ma, red), the target crust for the 56-Ma transect. Gray shading = seafloor depths >5000 m. F.Z. = fracture zone.

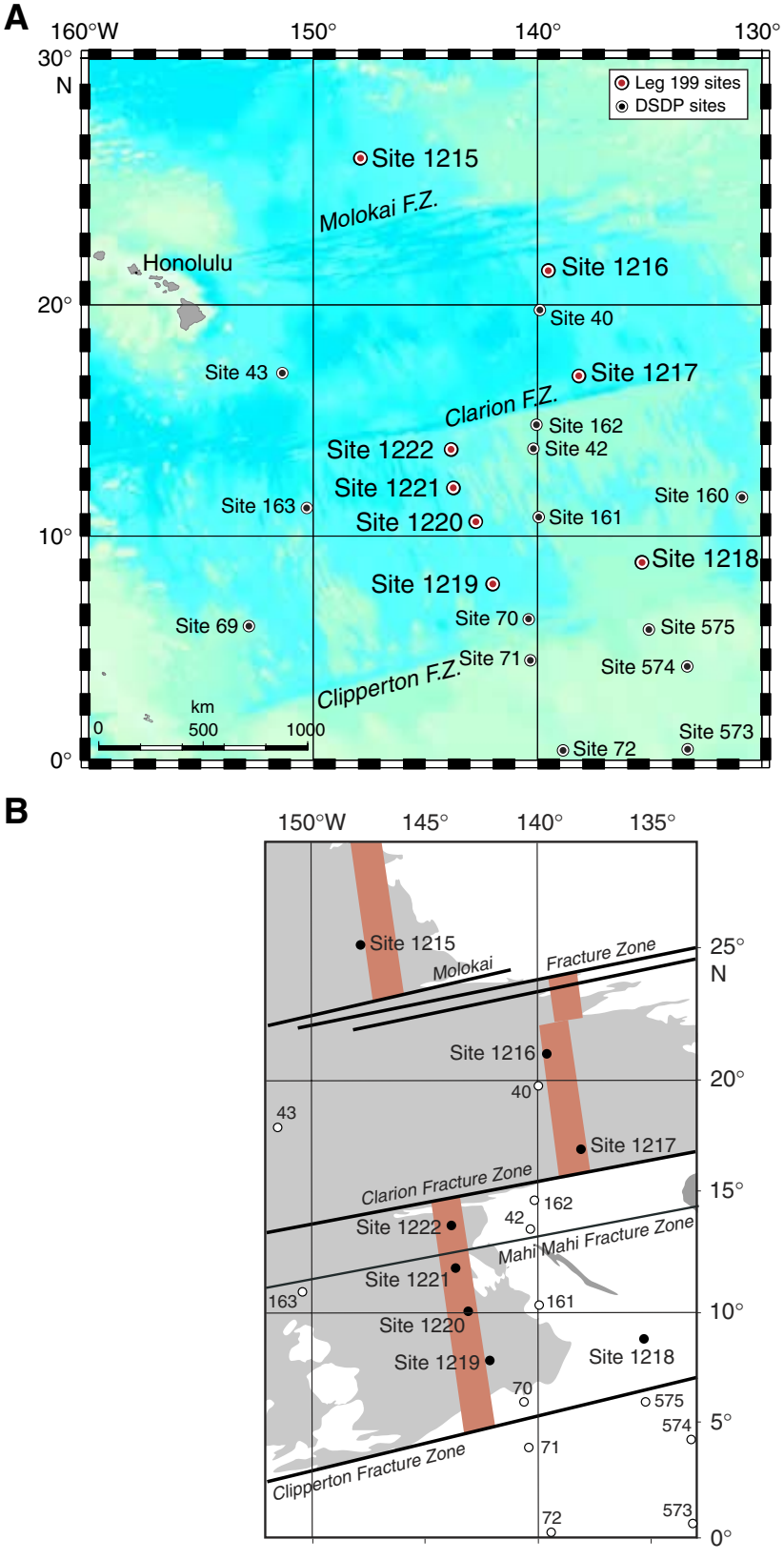

Figure F4. A comparison of shipboard VGP (virtual geomagnetic pole) latitude from shipboard paleomagnetics to those from the U-channel splice made postcruise (after Lanci et al., 2004). Data are from lower Miocene sediments of Site 1218. Although the shipboard paleomagnetic record was good, postcruise U-channel studies allowed the search for paleomagnetic events with lifetimes <20 k.y.

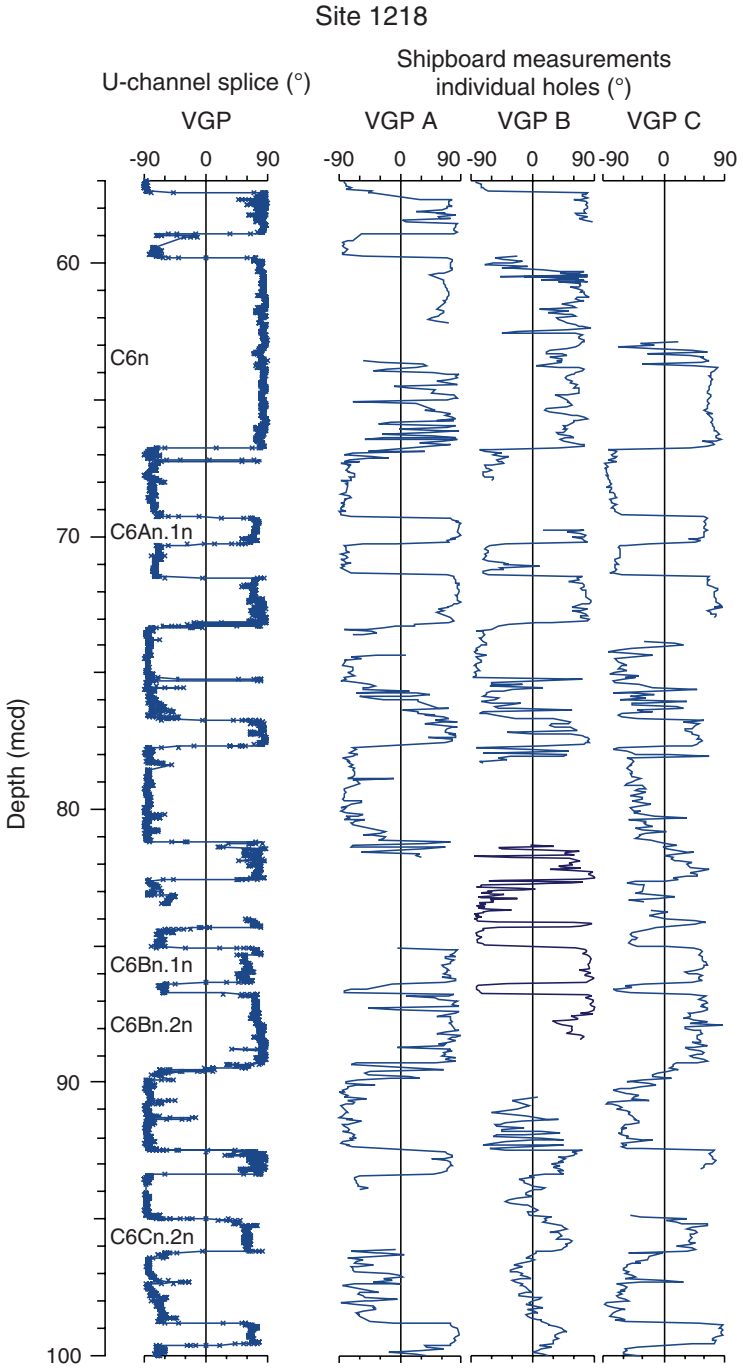

Figure F5. Comparison of estimated ages of radiolarian zones (Sanfilippo and Nigrini, 1998) to age boundaries intercalibrated with magnetic reversal stratigraphy during Leg 199. Leg 199 studies resulted in the first intercalibration of magnetostratigraphy and low-latitude radiolarian biostratigraphy and have significantly improved zone boundary ages and ages of individual fossil first and last occurrences (see **Nigrini et al.,** this volume).

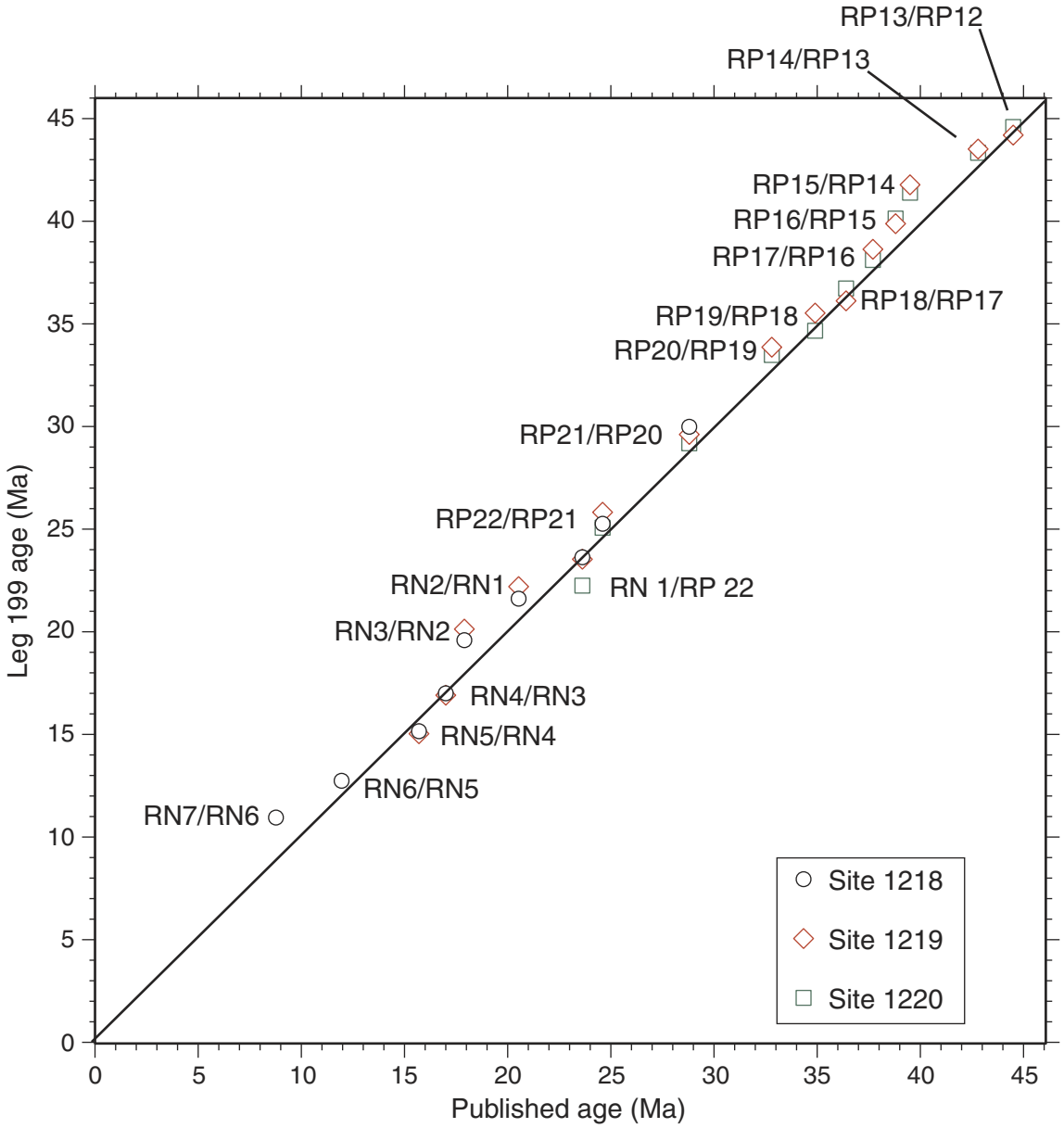

Figure F6. A comparison of primary productivity (top) vs. bulk mass accumulation rate (bulk MAR) for a modern transect across the equatorial Pacific at ~140°W (after Murray et al., 1993). The bulk MAR shows the same latitudinal pattern as productivity because the vast majority of the sediment is composed of remains of plankton.

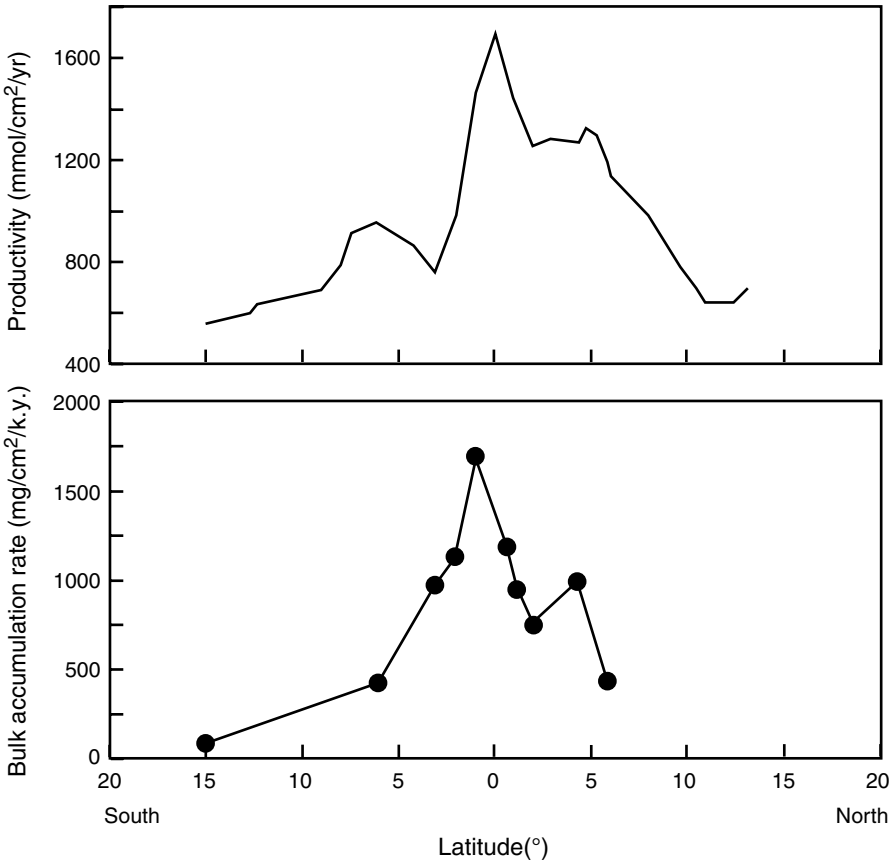

Figure F7. Chlorophyll contents in the Pacific equatorial region, from SeaWIFS imagery, September 1997–July 1998 composite. Chlorophyll content of surface waters correlates with high primary productivity. The position of the high-productivity (light colored) band along the equator is constrained by the change in sign of coriolis force at the equator and is a stable feature of the Cenozoic Pacific. Red = highest chlorophyll contents, Purple = lowest chlorophyll.

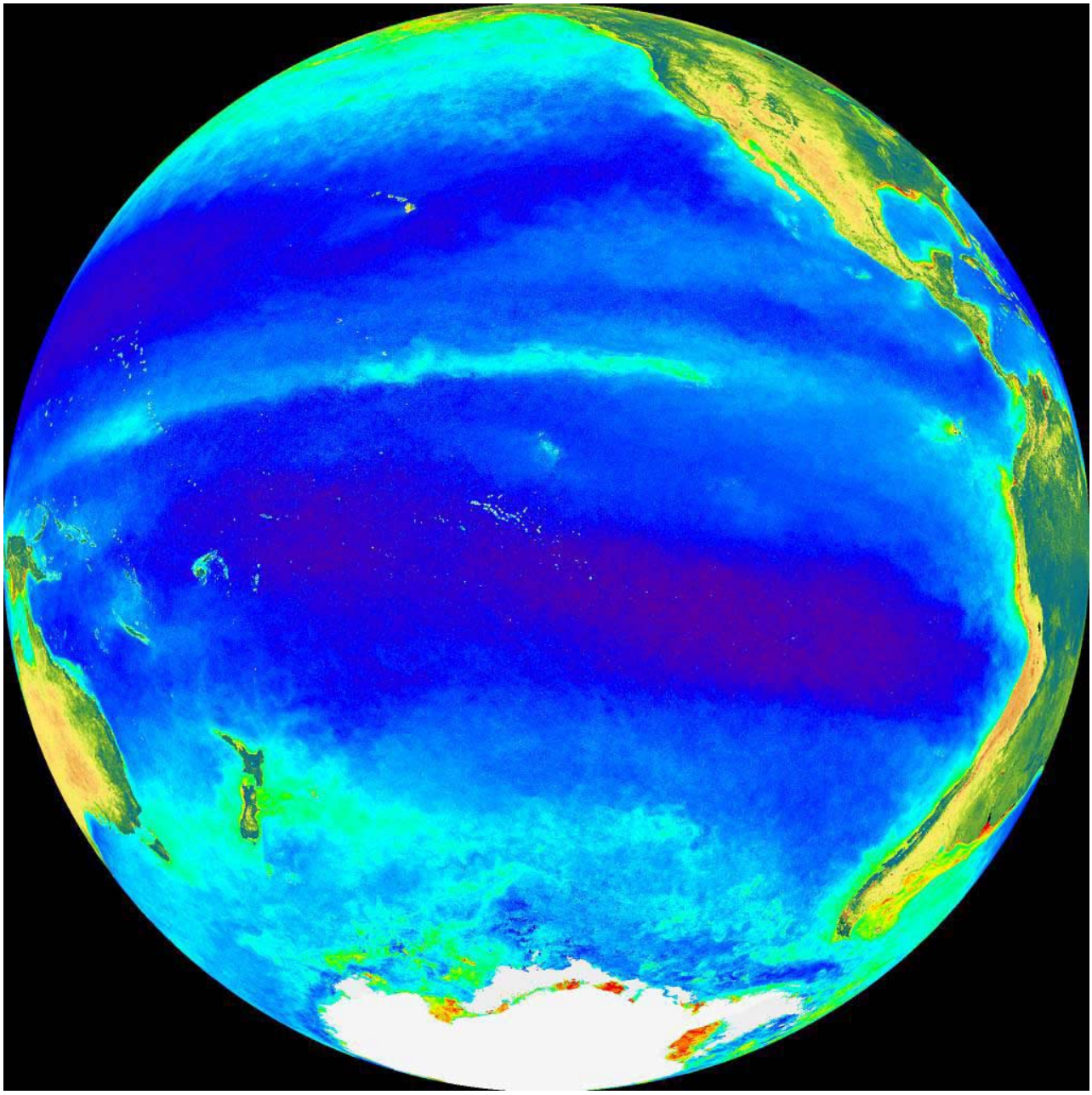

Figure F8. Average sedimentation rates in the tropical Pacific for the late Eocene time slice (m/m.y., 34–40 Ma) (after Moore et al., 2004). Sites are rotated to their estimated paleoposition at 37 Ma using a fixed-hotspot model for Pacific plate motion. Because the sediments primarily consist of tests of plankton, the sedimentation rates are a semiquantitative measure of paleoproductivity. Note that a well-organized zone of productivity exists at ~10°N in the late Eocene. Modern productivity in the region is lower and more poorly organized, as is shown in Figure F7, p. 34. Blue squares = ages estimated by carbonate microfossils, green inverted triangles = ages estimated by carbonate and siliceous microfossils, red triangles = ages estimated by siliceous microfossils, brown circles = sparse microfossils or clay. The red dashed line marks the approximate center of the equatorial divergence, or geographic equator.

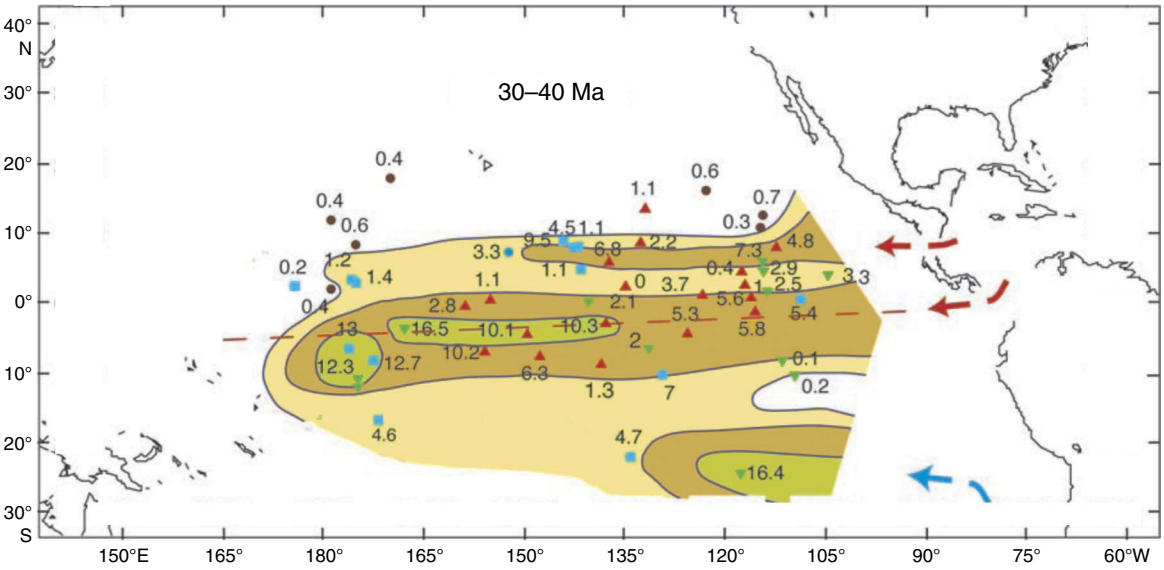

Figure F9. Subsidence histories for (A) nonequatorial Leg 199 sites (1215, 1217, and 1221) and (B) equatorial Leg 199 sites (1218, 1219, and 1220). Carbonate compensation depth (CCD) based on presence/absence of carbonate, from shipboard observations (from Shipboard Scientific Party, 2002). See **Lyle et al.** (this volume) for an updated study of the Eocene CCD, and see Coxall et al. (2005) for a more detailed study of the Eocene–Oligocene transition.

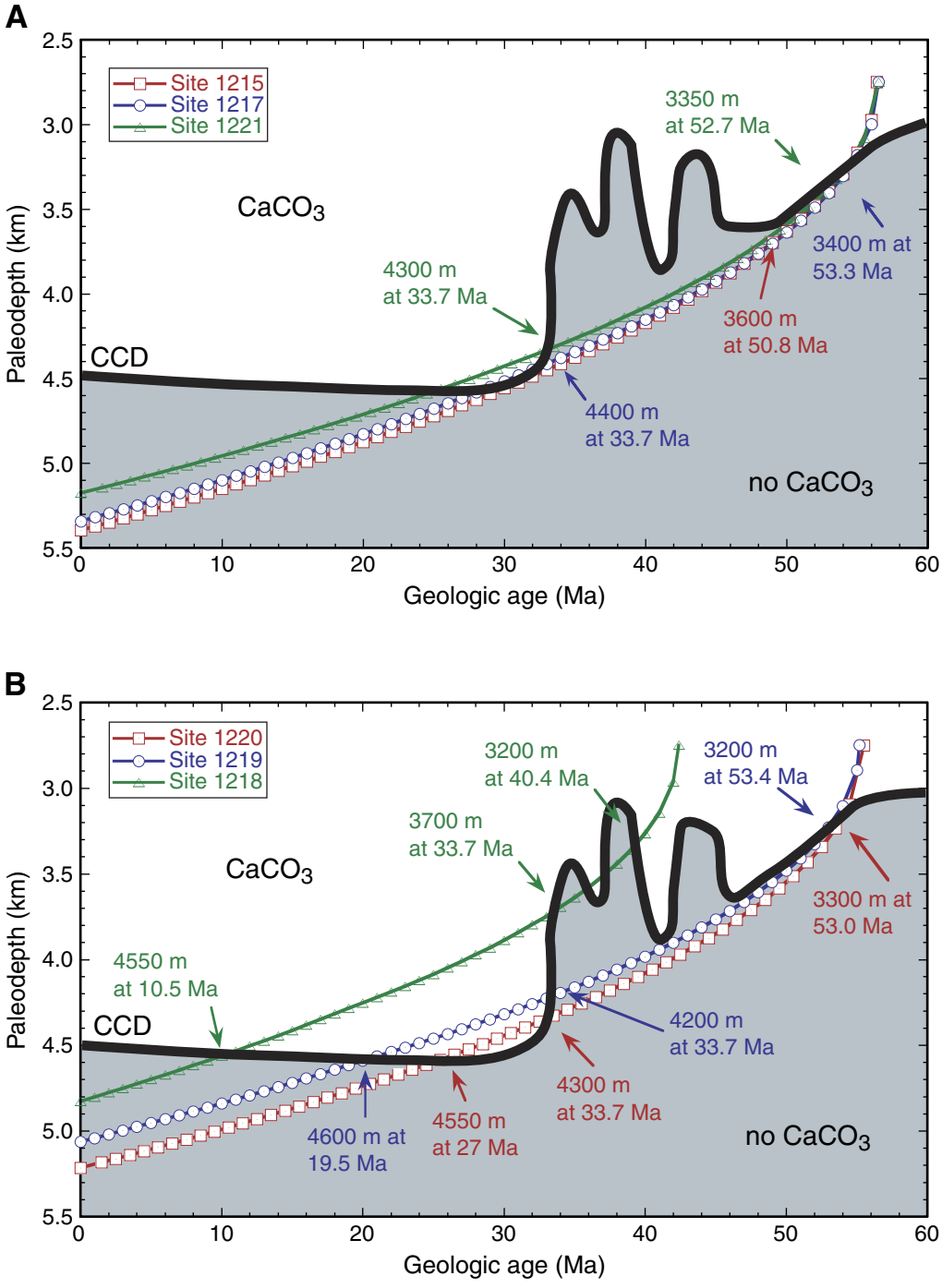

Figure F10. Digital images of the P/E boundary sediments recovered at Sites 1220 and 1221 (from Shipboard Scientific Party, 2002). Lower Eocene calcareous chalks grade downcore into multicolored clay-rich lithologies. The black layer in the center of the section is a manganese oxide–rich unit. The last occurrence (LO) of Paleocene benthic foraminiferal fauna is recorded at the base of the brown clay, and the first occurrence (FO) of Eocene assemblages is at the top of the dark brown clay. Calcareous fossils are barren to poorly preserved in the multicolored clay layers, where carbonates are very low to absent.

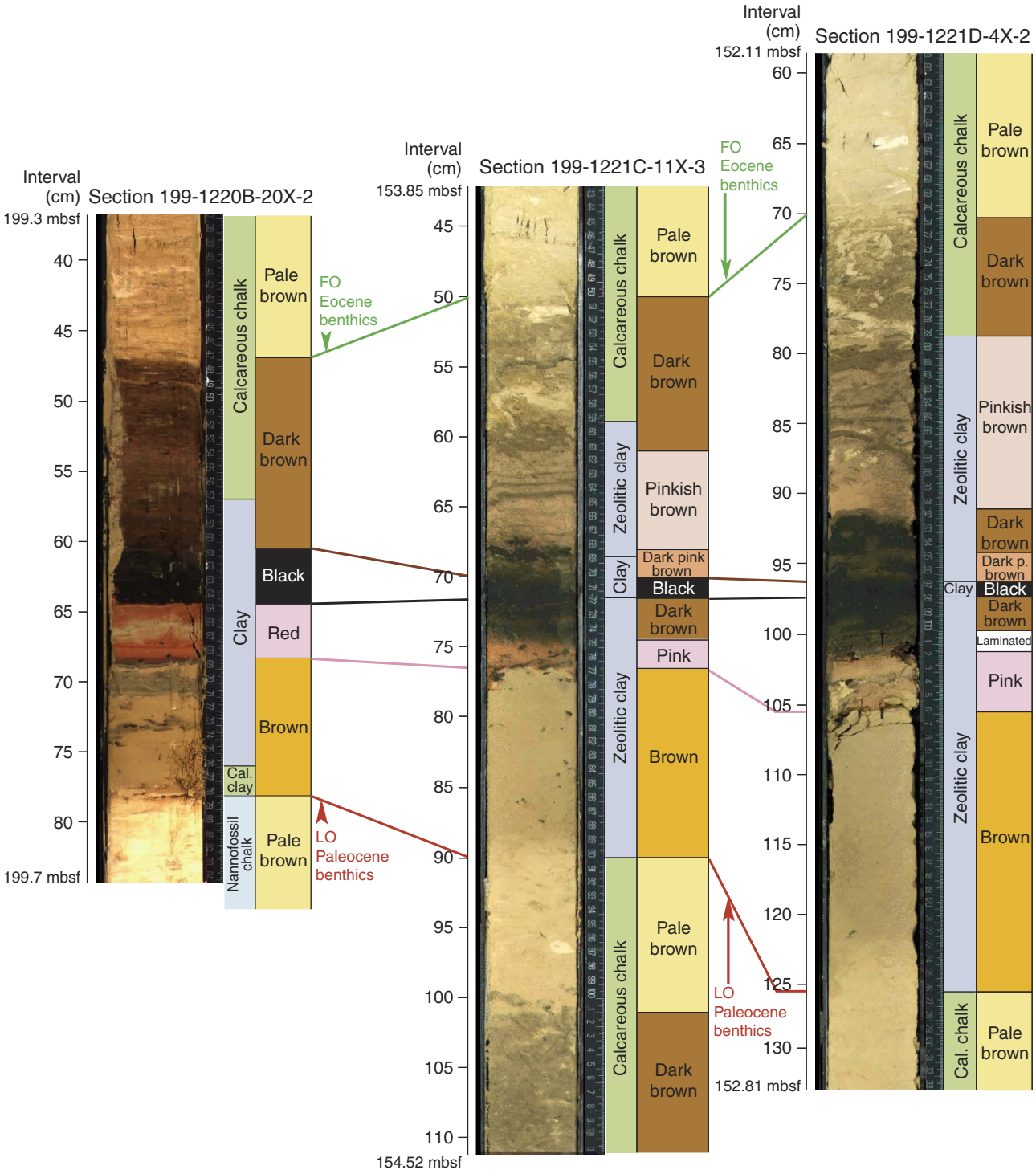

Table T1. Leg 199 site locations.

Site	North latitude	West longitude	Water depth (m)	Basal age (Ma)	56-Ma paleolatitude*	Sediment thickness (m)
1215	26°01.77′	147°55.99′	5395	56.2	11.5°N	70
1216	21°27.17′	139°28.79′	5150	—†	9.0°N	>62
1217	16°52.02′	138°06.00′	5342	54.5(?)	4.9°N	138
1218	08°53.38′	135°22.00′	4827	42	—	263
1219	07°48.01′	142°00.94′	5063	54.5	–4.8°N	250
1220	10°10.60′	142°45.50′	5218	55.5	–2.8°N	202
1221	12°01.99′	143°41.65′	5175	56.2	–1.1°N	153
1222	13°48.98′	143°53.34′	4989	55(?)	1.0°N	98

Notes: * = fixed hotspot model. † = drilling did not reach basement. — = no data.

CHAPTER NOTES*

N1. Pälike, H., Norris, R.D., Herrle, J.O., Wilson, P.A., Coxall, H.K., Lear, C.H., Shackleton, N.J., Wade, B.S., and Tripati, A.K., submitted. The heartbeat of the Oligocene climate system. *Science*.

N2. Lyle, M., Barron, J., Bralower, T.J., Huber, M., Olivarez Lyle, A., Ravelo, A.C., Rea, D.K., and Wilson, P.A., submitted. The Pacific Ocean and the Cenozoic evolution of climate. *Rev. Geophys*.

*Dates reflect file corrections or revisions.